2-1-2016

Magnetic Switches as Active Device Replacements for Harsh Environments

Joshua A. Gilbrech

Joshua A. Gilbrech

Candidate

Electrical and Computer Engineering

Department

This thesis is approved, and it is acceptable in quality and form for publication:

Approved by the Thesis Committee:

Edl Schamiloglu , Chairperson

Jane Lehr

Sarita Prasad

Magnetic Switches as Active Device Replacements for Harsh Environments

BY

Joshua A. Gilbrech

Bachelors of Science, Electrical Engineering

THESIS

Submitted in Partial Fulfillment of the
Requirements for the Degree of

Master of Science

Electrical Engineering

The University of New Mexico
Albuquerque, New Mexico

December 2015

DEDICATION

To my Mother, who taught me the importance of learning something new every day in life, my sister who has provided a constant competition and an endless sounding board, and finally to my wife who is always there to motivate and support me in finishing what I've started.

ACKNOWLEDGEMENTS

First off I would like to acknowledge Tetra Corporation for supporting continuing education. To William Moeny especially, the constant encouragement to continue seeking, studying, and asking questions are part of what made this possible. Thanks to Dr. Prasad for random coffee brainstorming sessions. Thanks Dr. Schamiloglu for serving as chairperson of my committee. Thanks to Dr. Lehr for being a late saving grace. A very special thanks to the late Jeff Oicles for setting me on the yellow brick road that is pulse power work. One final thanks to Dr. Richard Adler for an immeasurable amount of learning in an extremely short time. To all of you for making this happen.

Magnetic Switches as Active Device Replacements for Harsh Environments

By

Joshua A. Gilbrech

B.S., Electrical Engineering, University of Arkansas, 2004

M.S., Electrical Engineering, University of New Mexico, 2015

ABSTRACT

This thesis explores the use of the archetypical pulsed power magnetic switching devices in alternative and novel methods. The primary motivator for investigating these applications are for the purpose of simplifying electrohydraulic drill and electrocrushing designs meant for extreme environment operation, outside of the normal operating parameters of most switching technologies available to the modern electrical engineer. Since the nonlinear behavior of saturating magnetics allows a switch type action, a diode like behavior, and a delay type behavior, a number of architectures can be constructed from extremely robust and simplistic designs.

A number of these designs were simulated, built, and tested in the laboratory. These fully realized solutions are documented and explored herein. The designs were implemented on a 1-2 kJ pulse modulator built for the purposes of testing a number of effects on the drilling process. The modulator was built in a number of fashions in order to experiment with the various architectures made possible by this work. The proven designs were later implemented in a laboratory machine running extensive testing. These successful designs were based upon a parallel magnetic compression circuit, a magnetic diode circuit, a pulsed primary switch circuit, and a magnetic delay trigger circuit.

Further work utilizing nonlinear magnetics in the field of electrocrushing and electrohydraulic drilling is recommended, particularly where these components can replace devices that need cooling to

operate within their normal parameters. This technology proves useful in any system exposed to extremes of pressure and temperature.

TABLE OF CONTENTS

LIST OF FIGURES

APPENDICES

LIST OF TABLES

Chapter 1

Historical Background

The first description of the use of nonlinear magnetics for the purpose of creating a saturable reactor was documented by C.F. Burgess and B. Frankenfeld in 1903 [1]. Some of the figures from their patent can be seen in Figure 1.1. The basis for their patent "Means for regulating self-inductance in electrical circuits" was from an earlier patent of theirs titled, "Regulation of electrical circuits." While the earlier patent describes the use of nonlinear magnetics for the purpose of regulating AC waveforms, more of a magnetic amplifier, the second patent truly investigates the use of the B-H loop of magnetic material through saturation and how that characteristic could be utilized [2]. In "Magnetic Amplifiers: Theory and Application," Platt has an excellent analysis of early patent work from Frankenfeld and Burgess's first patent through all the patents listed on the technology to 1950 [3]. This list has been reproduced and is available in Appendix A.

A number of additional patents started showing up in the early 1950's. These were primarily concerned with the idea of being able to alter the inductance of a wound component without the need for rewinding the component. It turns out that World War II would be the catalyst for bringing this technology to the forefront of common electronics. The need for robust components that could operate in a myriad of harsh environments created a perfect opening for the use of saturable reactors and nonlinear magnetics. These techniques and technologies were used throughout communications, early radar, and control systems. Germany was quick to adopt the technology and utilized nonlinear magnetics in a variety of military equipment, from mines to early autopilot systems, and to early guided missile systems such as the V1 rocket.

This spur of military use allowed magnetic core material to mature and catch up to the techniques theorized before the 1950's. Mass production methods of manufacture were applied to cores and windings such that the homogeneity of nonlinear devices could be used in mass assembled products.

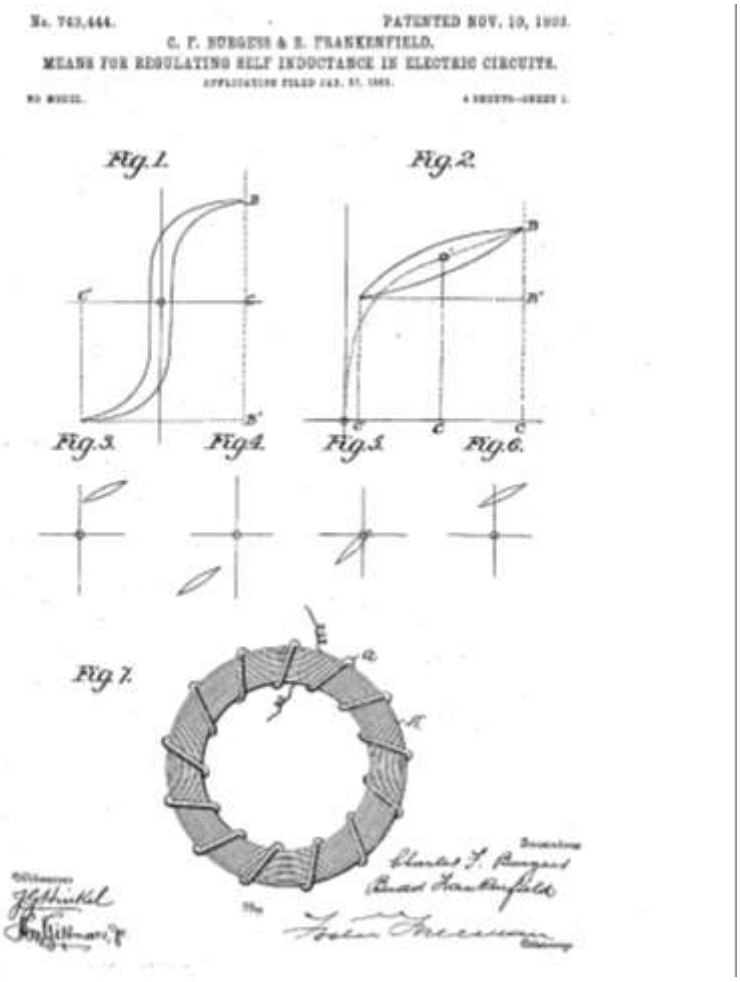

Figure 1.1 First documented patent for nonlinear inductive effects [1].

1-1 Downhole Operations

Downhole[1] operations are a burgeoning field in today's marketplace. When oil and gas prices reach critically high values the economics of drilling in new markets changes. These changes elicit research and development to make use of these sites where traditional drilling methods are unable to support a profitable well. With this influx of money come opportunities in the form of new problems to solve; many of these problems have solutions based in pulsed power technologies. The true difficulty with solving these problems is in turning a laboratory proof-of-principle device into a field worthy test system that can operate in the downhole environment. The purpose of this chapter is to investigate technologies for use in high temperature and high pressure pulsed power applications. The general range of interest is contained within 125-250º C. Of secondary interest is the ability of these technologies to withstand increased pressure conditions, pressures in excess of 1,000 PSI without extreme efforts being utilized to allow for their use. An investigation into applicable technologies and devices commonly utilized in the field of pulsed power shall follow.

1-2 Vacuum Tubes

Vacuum tubes are the standby of pulsed power systems. They are capable of delivering the extremely high instantaneous powers that are required for pulsed power system architectures. The baseline for most systems requires operation in the tens of kV and thousands of Amps range. Vacuum tubes are limited thermally only by packaging. From a packaging standpoint the critical characteristic is the gas seals on the tube that connect the various electrodes to the ceramic or glass insulators. The typical metal-to-ceramic seals present in most devices are created in

[1] Downhole in the oil industry denotes any piece of equipment that is used in the oil well itself.

furnaces that operate at 1,500º C. This allows for normal operation up to and beyond 300º C. Increases in ambient temperature do not affect the overall lifetime of the device [4]. This allows numerous options for systems that function within pulsed tube operating areas.

1-3 Solid State

Solid state technology can replicate vacuum tube operation in a very select operating area by a single device. In order to extend this operating area it is necessary to series/parallel devices to mimic vacuum tube operation. The challenge with operation in this mode is the requirement of additional ancillary circuitry for each device added to the series/parallel combination. There are a number of companies currently producing thyratron replacement solid state systems [5-8]. The goal and challenge of these systems are to create a device that can deliver the same performance with equal reliability at extended lifetime comparable to that of a vacuum tube solution. The equal reliability part of the equation is the challenge of the moment. Vacuum tubes can operate in a complete fault mode and recover with little detriment to the lifetime of the device. The drawback of a solid state system is that complete fault modes typically end with the requirement of replacing the device stack. This makes it critical for the system designer to over rate devices and build in a large safety margin in the system design. In addition to this, the nature of pulsed power loads is such that they typically tend towards lower impedance, high voltage output waveforms and it can be difficult to distinguish these output waveforms from that of a short circuit. Thus, protection networks and control schemes must be able to protect the system in sub-microsecond timescales to ensure device survival. These circuit designs must include methods that turn hard failures into soft failures, further increasing the system complexity and size. Figure 1.2 illustrates a solid state crowbar replacement system used at CERN [6]. As one can see, a similar sized solution is also presented in the figure. What is not shown, however, are the heater

and reservoir transformers for the thyratron based solution. In terms of weight, the elimination of these can be a great savings; however, the size of the controls and gate drives for most solid state solutions typically make for the real estate trade off being a net zero change.

Figure 1.2 Solid replacement for a thyratron switch [6].

Operating any solid state component at elevated temperatures is a complex problem. Depending upon how the component is made, it is possible that a typical 85º C part is capable of running at temperatures beyond 150º C [9]; however, this is not usually the case and problems often arise from running components at elevated temperatures. These problems range from wire bonding failing due to the melting of solder at the bond, caustic chemicals being generated from packaging failure resulting in massive failure at multiple points, to even basic issues such as the junction of the device itself not being able to handle the ambient heat. Even if one manages to get a device rated for operation above 150º C there are all the other ancillary passive components necessary for circuit operation (resistors/capacitors/inductors).

The more components one adds to any circuit means that the probability of a single failure grows. Increasing the temperature at which components operate decreases the mean time to failure. This all aligns to the need for circuit designs created for operation at elevated environmental levels to be designed to a bare minimum in terms of features and operating parameters. Essentially, the design acknowledges that parts will fail, and designers are trying to get the most life out of their system. This of course flies in the face of designing a system based around a solid state solution. In order to get to the design parameters necessary for most pulsed power systems a multitude of components are required to create a single switch. There is, however, hope in the prospect of new device technology on the horizon.

At present, silicon-based devices are the primary commercially available option. Silicon carbide (SiC) technology is finally reaching a level at which designers are starting to see components become available commercially. More interestingly, SiC technology shows great promise pulsed power applications in particular [10]. At the device properties listed in [10], it would be relatively easy to accomplish a thyratron replacement system out of a handful of devices. One attractive characteristic about SiC technology is that, whereas silicon devices are limited to a junction temperature of 150º C, the theoretical limit on SiC devices is close to 600º C. Designs have already been created that operate these devices at or beyond 200º C without negative effect to the circuit [11].

Another promising material is gallium nitride [12]. Gallium nitride has higher electron mobility than SiC or traditional silicon and has a maximum junction temperature similar to that of SiC. As such, it shows promise for higher frequency RF pulsed power applications. A list of device properties is shown in Table 1. SiC, however, has a higher breakdown field rating which makes it more attractive for higher voltage device applications.

Table 1. Device material properties [9].

Material	Mobility, μ, $cm^2/V.s$	Dielectric Constant, ε	Bandgap, Eg, eV	Break down field, Eb 10^6V/cm	BFOM Ratio	Tmax, ^oC
Si	1300	11.9	1.12	0.3	1.0	300
GaAs	5000	12.5	1.42	0.4	9.6	300
4H-SiC	260	10	3.2	3.5	3.1	600
GaN	1500	9.5	3.4	2	24.6	700

1-4 Nonlinear Magnetics

Nonlinear magnetic systems are another well-used archetype in pulsed power. Typical systems used involve utilizing the nonlinear behavior of core material to illicit a switching action. In this mode, a typical wound core inductor can be made to have a high impedance (OFF) state and a low impedance (ON) state, a saturable reactor. Utilizing a number of stages, when designed properly, this will allow for a compression of the initial pulse. This can be used to increase the voltage and/or the current of the output pulse while lowering the output waveform's pulselength. This is best illustrated by Figure 1.3 [13]. Large pulsed power systems, such as the RHEPP machine, have been driven entirely by an AC source, lacking anything other than magnetic saturable reactors [14].

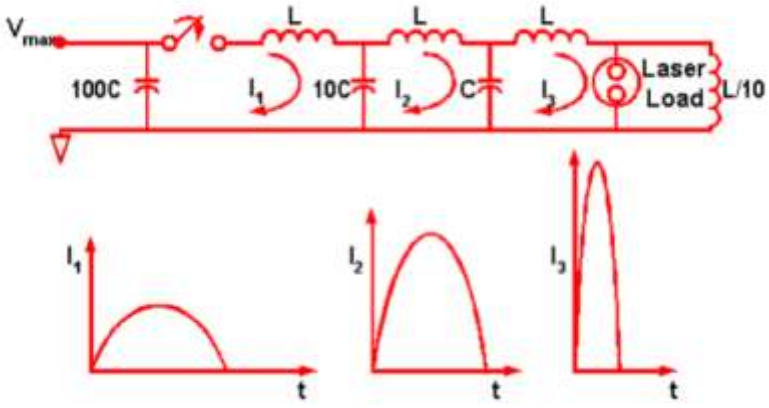

Figure 1.3 Pulse compression using nonlinear magnetics [13].

Because the switching action is accomplished with simply a wound device, one only has to make sure that the wire and the core material are rated for operation at ambient temperature. This does involve some consideration when it comes to the core material, as a number of core types that are typical to use in this architecture suffer in elevated temperatures [15]. From the observations in the previous reference one can see that most of the core types suffered a significant loss in Brem and Bmax once the core material was taken up beyond 200º C, Figure 1.4. Brem is the remanent magnetic field and Bmax is the maximum magnetic field in the B-H curve. However, the Supermendur material has little loss in those ranges and even shows an increase in AC coercive force. The magnetic amplifier is a design relegated to history [3]. Well-utilized for its ruggedness in the past, it has been replaced with more modern IC technology control schemes.

The basic operation of the magnetic amplifier is as follows: Envision an inductor in line with the load. This inductor has an AC winding and a control winding. As one adjusts the control winding one can affect a change in the AC impedance on the AC winding, thus allowing more or less current to flow through the winding. Figure 1.5 illustrates the basic schematics for magnetic amplifiers, both AC and DC. One could envision in the AC version replacing the AC source with a transient pulse, allowing the gating of this pulse (with proper timing and control) to generate a required output waveform. With the correct topology and core material selection one could utilize this output to discharge a resonantly or impulse charged storage capacitance, essentially creating a meld of the typical saturable reactor system and the magnetic amplifier topology.

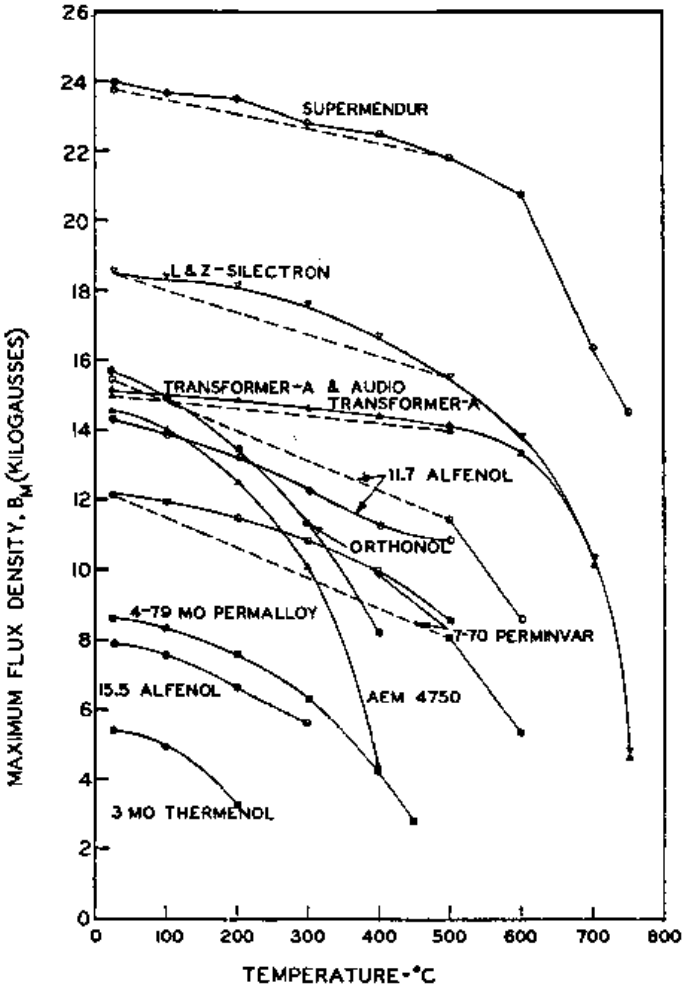
MAXIMUM FLUX DENSITY, B_M (KILOGAUSSES)
TEMPERATURE - °C
SUPERMENDUR
L&Z-SILECTRON
TRANSFORMER-A & AUDIO
TRANSFORMER-A
11.7 ALFENOL
ORTHONOL
4-79 MO PERMALLOY
7-70 PERMINVAR
15.5 ALFENOL
AEM 4750
3 MO THERMENOL
0
2
4
6
8
10
12
14
16
18
20
22
24
26
0
100
200
300
400
500
600
700
800

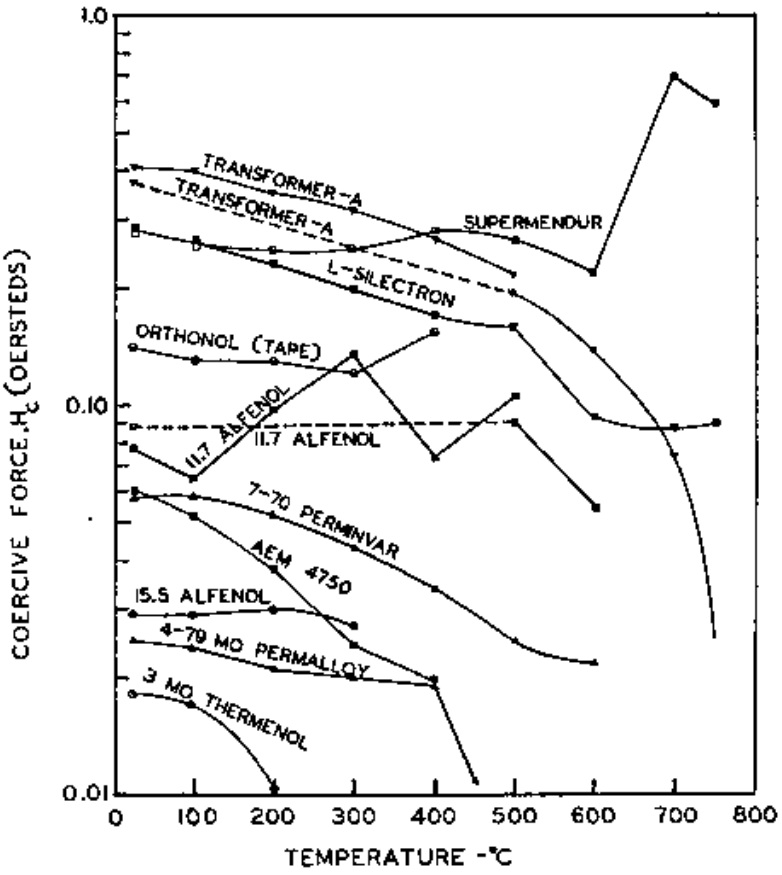

Figure 1.4 Effects of thermal cycling on characteristics of magnetic materials [15].

Alternate options exist for pulsed power generation utilizing LC circuits. Most of these systems rely on series or parallel resonance to generate high voltage. The Nested High Voltage Generator (NHVG) is a good example of a system that employs a resonant high voltage drive for various loads. The high voltage generating part of this system is typically a single or double resonant Tesla transformer that drives a Cockcroft-Walton voltage multiplier. The multipliers are arranged in individual pucks that grade the voltage throughout the system structure and add their generated voltage to each other in a series fashion. The output of these systems are varied, capable of generating high voltage pulses with an integrated output switch, or an ion/electron beam through an integrated accelerating column. This system has also already been successfully

deployed downhole for well logging applications [16]. Figure 1.6 shows a sample NHVG build and basic schematic [17]. Nonlinear magnetic systems are another well used archetype in pulsed power.

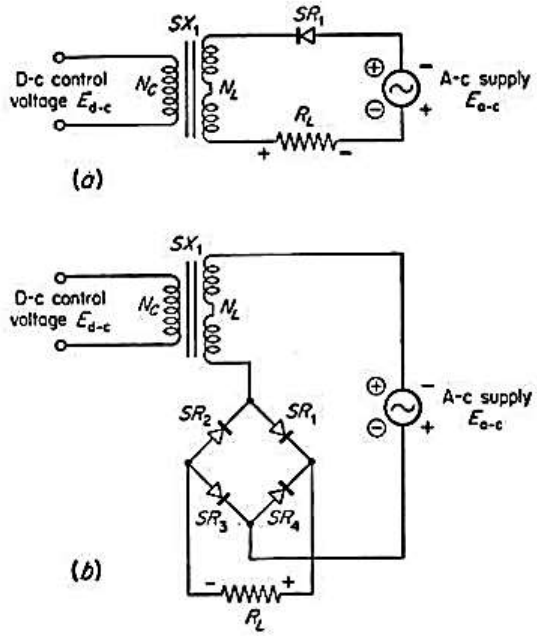

Figure 1.5 Basic schematics for a magnetic amplifier [3].

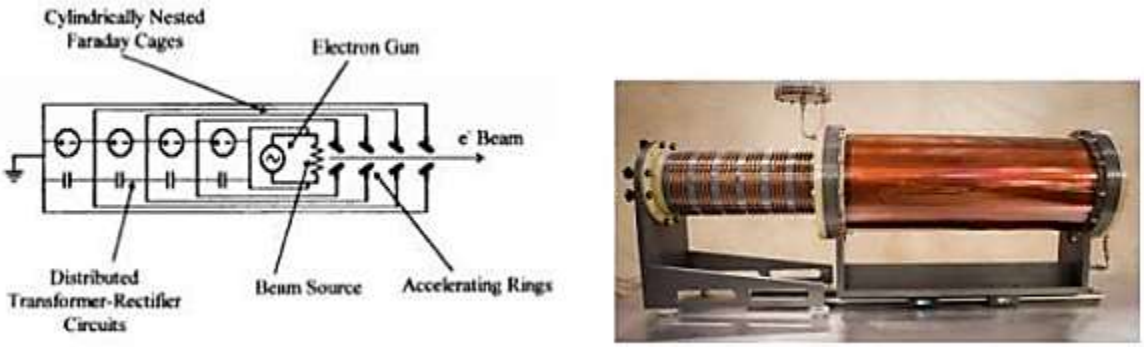

Figure 1.6 NHVG schematic and build [17].

1-5 Ambient Pressure Considerations

A secondary consideration is that of pressure effects on these devices and architectures. Solid state devices have the benefit that as long as the devices are impregnated fully they are immune to pressure effects. This means that for most types of devices except for larger modules the devices would be able to meet the pressures in excess of 1,000 PSI. Larger module type devices would need to be vacuum-encapsulated in such a way as to eliminate voids and encapsulated with material that would be impervious to the stresses associated with the elevated pressure circumstances.

As shown in the earlier Beckwith reference, extensive time and testing is required for a solid state solution to be employed successfully downhole. Every part of the circuit must be individually verified and or specially designed to cope with the environmental concerns, even when placed in a specially designed protection bottle. Alternatively, one could encapsulate the whole assembly as long as special care is taken to remove the heat generated by circuit operation. Because the designs of a solid state solution are typically modular in nature operation in downhole dimensions can be less challenging than for other solutions. Vacuum based devices are capable of withstanding elevated pressure only with extensive effort. Essentially, the device would need to exist in a separately designed pressure bottle. Such a bottle would need to incorporate high voltage feedthroughs, and heater/reservoir feedthroughs, and it would also need to be able to conduct the thermal losses associated with operation out of the bottle in such a way as to maintain internal pressure while not putting additional pressure on the assembly. These aspects to designing a pressure capable vacuum device do not eliminate it from possibility; however, they vastly add to the difficulty and expense of employing this technology as a solution.

Size begins to play a very important role as the vacuum tube solution starts to grow ponderous as multiple layers of protection are required to ensure its operation in the hostile environment. Magnetics based devices would be impervious to the effects of pressure due to a lack of trapped gases incorporated into the device structure. Given this, the device could operate at ambient pressure with few, if any, negative effects.

Pulsed power systems are often large laboratory machines described as solutions looking for problems. One of the most challenging problems presented to the pulsed power engineer is to find a way to bring these systems out of the laboratory and into often-harsh environments. Such harsh environments often have volumetric and/or weight requirements which limit the options for system architecture and device selection. The prospect of putting a system downhole is a daunting one. It compounds the ever present aspects of the problems associated with creating a field-worthy system to the unique problems involved with downhole systems. Elevated temperature and pressure are the most obvious aspects that are covered here; however, some less obvious ones were not, such as dealing with cable lengths in excess of thousands of feet.

1-6 Summary

The research performed for this thesis has evaluated a number of options for systems that would be used in the downhole environment where elevated ambient pressure and temperature are present. Each of these options brings its own challenges and solutions to the problem. One thing is for certain: the more simplistic a system can be the more rugged it will be in every situation. The design equation must be rebalanced so as to treat the system as a very expensive disposable solution.

This thesis describes the use of magnetic switches for pulsed power systems for downhole applications. The rest of this thesis is organized as follows. Chapter 2 discusses resonant energy transfer and nonlinear magnetics calculations. Chapter 3 discusses simulations of four applications of magnetic switching. Chapter 4 describes simulations of these four circuits. Chapter 5 describes the construction of these four circuits. Chapter 6 describes the testing results of the four constructed circuits. Finally, Chapter 7 discusses conclusions drawn from this Thesis. Appendix 1 and Appendix 2 cover early patents concerning nonlinear magnetics and application of the Jules-Atherton SPICE model, respectively.

Chapter 2

Theory of Operation

2.1 Resonant Energy Transfer

The C-L-C energy transfer, or resonant energy transfer, is an effective, efficient method of transmitting energy from one energy storage device to another. As such, it is commonplace in some form or fashion in most pulse power systems. The very basic topology for this circuit is shown in Figure 2.1.

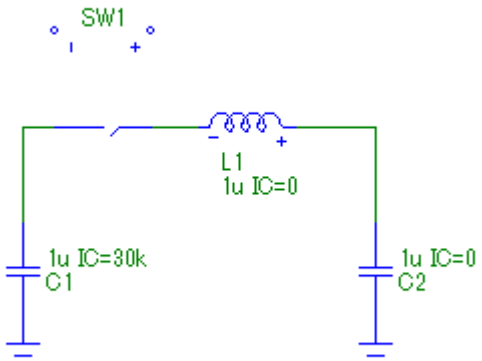

Figure 2.1. A C-L-C circuit.

In this circuit, energy transfer occurs when SW1 closes. This allows the voltage in C1 to oscillate through L1 and charge C2. The simulation of this process can be seen in Figure 2.2, where the bottom trace is the current and the top traces are the voltages on C1 and C2.

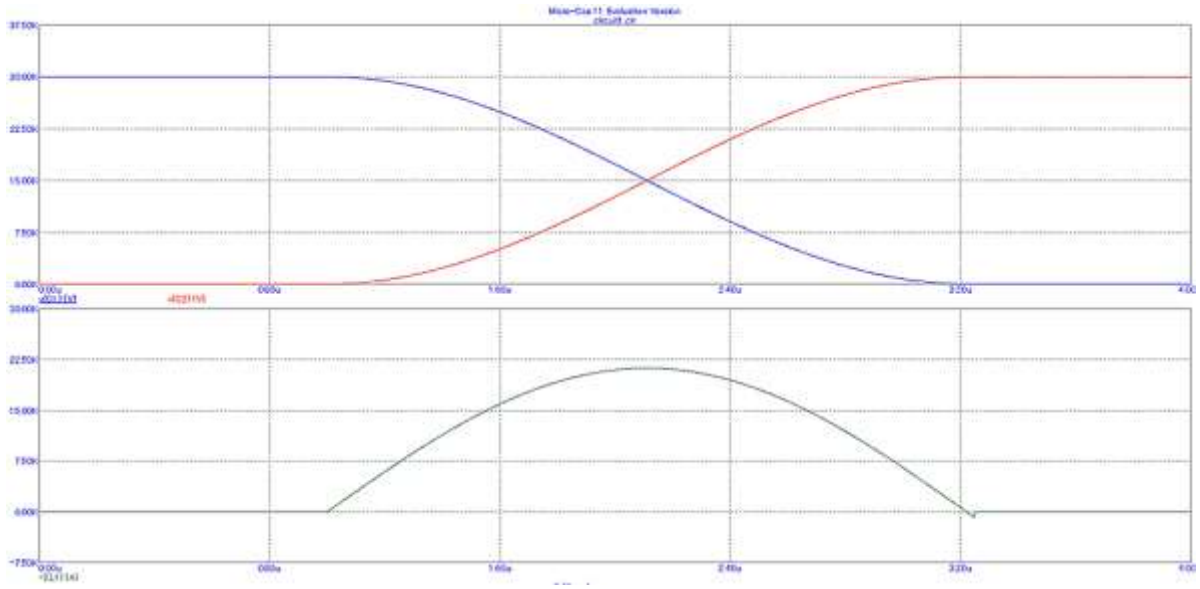

Figure 2.2. Resonant energy transfer between two equivalent capacitances.

The current that travels through L1 is defined by:

$$I(t) = \frac{\omega_0 V_0}{\frac{1}{C_1} + \frac{1}{C_2}} \sin \omega_0 t \tag{2.1}$$

This current oscillates through L1 as defined by the period defined in 2.2. The voltage that capacitor C2 charges to can be calculated utilizing Eqs. (2.3-2.4). As shown here one can utilize a mismatched set of capacitances to increase the voltage to which C2 charges. This gain is at the cost of efficiency of the overall energy transfer, as shown in Eq. (2.5).

$$\omega_0 = \sqrt{\frac{1}{L}\left(\frac{1}{C_1} + \frac{1}{C_2}\right)} \tag{2.2}$$

$$V_{c2}(t) = \frac{V_0}{1 + \frac{C_2}{C_1}}\left[1 - \cos \omega_0 t\right] \tag{2.3}$$

$$V_{c2}\max = \frac{2V_0}{1+\frac{C_2}{C_1}} \tag{2.4}$$

$$\eta = 4\frac{\frac{C_2}{C_1}}{\left(1+\frac{C_2}{C_1}\right)^2} \tag{2.5}$$

2.2 Nonlinear Magnetics

Any device that makes use of nonlinear saturating magnetics must be based on a ferromagnetic core. Thus, our equations for analysis and design are derived from the Maxwell-Faraday equation

$$\nabla \times \mathbf{E} = -\frac{\partial \mathbf{B}}{\partial t} \tag{2.6}$$

This brings us to the integral form of Kelvin Stokes theorem

$$\oint_{\partial\Sigma} \mathbf{E} \cdot d\boldsymbol{\ell} = -\int_{\Sigma} \frac{\partial \mathbf{B}}{\partial t} \cdot d\mathbf{A} \tag{2.7}$$

If B is not = f(A) then for Nt turns, V= -Ac*Nt*dB/dt where Ac is, the core cross-sectional area, and Nt represents the number of turns. For resonant energy transfer we are more concerned with the Vt required as per the applied C-L-C energy transmission. For our case we will consider both C's in the equation to be equal for simplification.

$$V_C(t) = V_O \cdot \left(1 - \cos\omega \cdot t\right) \tag{2.8}$$

$$\int \frac{V_C(t)}{N_T} dt = \frac{V_O}{N_T} \int_0^{T_{SAT}} \left(1 - \cos\omega \cdot t\right) dt = A_c \cdot \Delta B \tag{2.9}$$

$$A_c = \frac{V_O \cdot T_{SAT}}{2 \cdot \Delta B \cdot N_T} \tag{2.10}$$

$$\omega_0 = \frac{1}{\sqrt{LC}} \tag{2.11}$$

Ideally, the designer has both L and C already in mind during the design. As such one now needs to figure out how to get to the saturated inductance L. The designer has two values that they can adjust this value, Nt and Ac. Earlier we calculated the required Ac for a set Nt. Nt and Ac both factor into the saturated inductance calculation as shown given by

$$L_{SAT} = \left(\frac{V_C \cdot T}{2 \cdot \pi}\right)^2 \cdot \frac{1}{E_T} = \frac{\mu_O \cdot \mu_{SAT} \cdot N_T^2 \cdot A_C}{x_M} \tag{2.12}$$

and

$$L_{SAT} = \left(\frac{V_C \cdot T}{2 \cdot \pi}\right)^2 \cdot \frac{1}{E_T} \tag{2.13}$$

Here Et is the pulse energy and T is the resonant period.

As shown in Eq. (2.12) Lsat scales as $(Nt)^2$. As such, it is more effective to adjust Ac to get to the required minimum Lsat and likewise adjust Nt upwards to get to the maximum required Lsat. Maximizing Nt versus Ac for a given design maximizes energy transfer efficiency as it minimizes leakage current during the hold off period. Figure 2.3 illustrates common square loop materials utilized for switching magnetics.

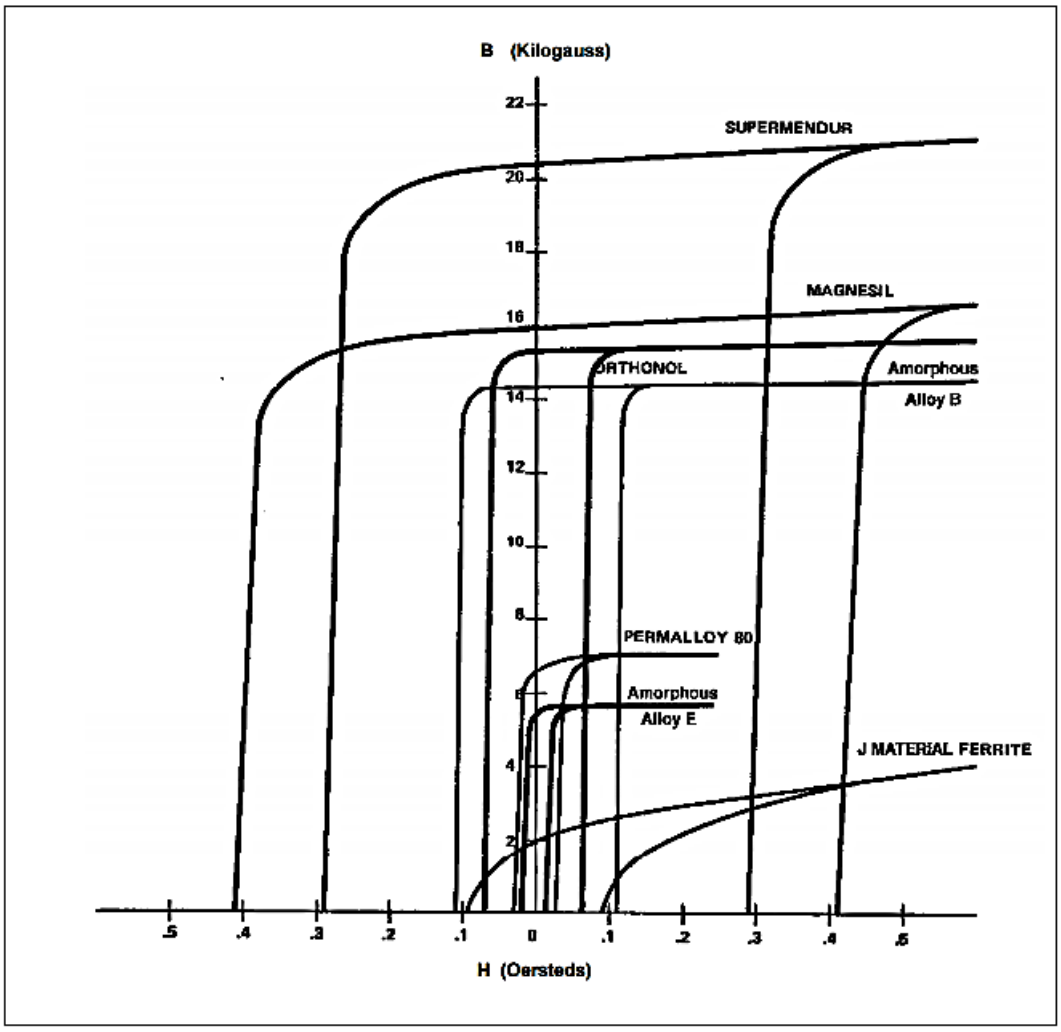

Figure 2.3 Common magnetic materials for nonlinear magnetic devices [18].

2-3 Summary

Resonant energy transfer is a common and efficient method of moving energy from one energy storage device to another. Using a magnetic switch to perform as the inductive element in circuits that this method of energy transfer is a natural choice as the device can act as both the inductive element and the switch. The prior sections have illustrated the equations needed to design and analyze a system using this circuit topology.

The next chapter discusses applications of nonlinear magnetic devices in common pulse modulator circuits. These options range from component level active switch replacement to subsystem trigger generation replacement.

Chapter 3

Practical Applications

3.1 Parallel Magnetic Compression

Parallel and series pulse compression lines offer a simplistic yet robust and reliable solution to many pulse modulator designs. For designs that do not rely on the compression of the pulse for output voltage gain, these systems can be extremely efficient as well. The designs for these machines are used throughout many pulse power solutions. For the designer's case at hand, a minimization of compression stages reduces component count, which, in turn reduces mean time between failure (MTBF) values. Since the system under consideration is expected to be operating in extremely hazardous environments in the future, the decision was made early on in the project timeline to minimize components where possible. As such, a parallel magnetic compression design was chosen for the initial prototype. The parallel magnetic compression topology allows for the saturation stages to incorporate traditional transformer impedance matching/voltage gain without losing energy in the ring up gain typical in a series type design.

For this particular application under consideration a parallel pulse compression system was designed. The pulse transformer, as illustrated in Figure 3.1, was designed with a Vt constant such that the transformer supported charging C2 to full energy transfer from C1 (see Figure 2.12). C3 is charged using an external pulse modulator that is inductively isolated from the secondary pulse. When the output gap closes C2 is drained and the transformer saturates, creating a low inductance path for the high energy storage of C3 to discharge into the load. This works much in the same fashion of striker/simmer circuits for flashlamp systems. The energy storage capacitor C3 is charged and designed for a low impedance load, while the main discharge

(high impedance) is supported by a low energy high voltage discharge through the pulse transformer.

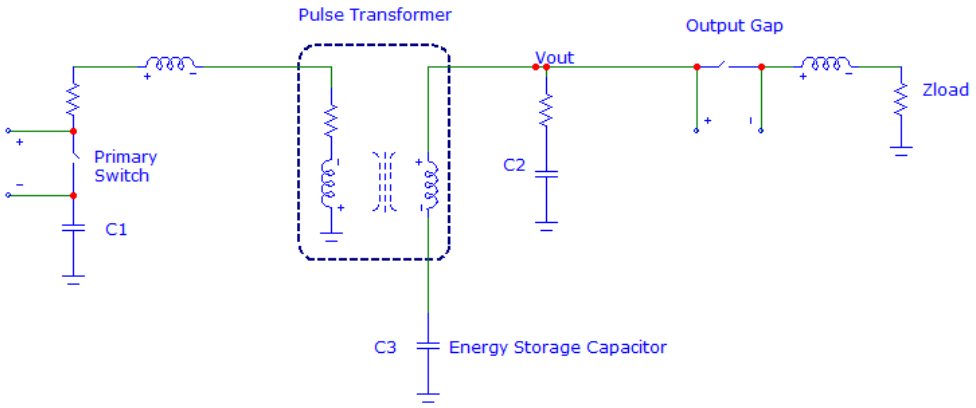

Figure 3.1 Saturating pulse transformer.

This works well for designs that do not incorporate a high turn ratio and/or short pulses. As the pulsewidth that the transformer has to support increases, the overall inductance of the primary and secondary increases. This increases the turns count, which increases the impedance of the saturated secondary windings. This can be supplemented or corrected by adding multiple windings to support the necessary impedance or peak current requirements at the cost of a more complex and expensive pulse transformer design and build.

3.2 Magnetic Diode

While there are some options for high temperature diodes in SiC, the range is slim and the price is high. Utilizing a magnetic switch in the mode of a temporal diode is an attractive alternative. This alternative is for a limited time in that the magnetic switch will impede current flow in one direction for as long as the Vt constant holds. The direction would be determined by the reset winding moving the B-H loop in one direction or the other to allow utilization of the full delta B (Brem+Bmax). Current flow in the opposite direction would be allowed due to the B-

H loop being set hard to that direction. Thus, the magnetics are always in a saturation mode for one direction of current flow.

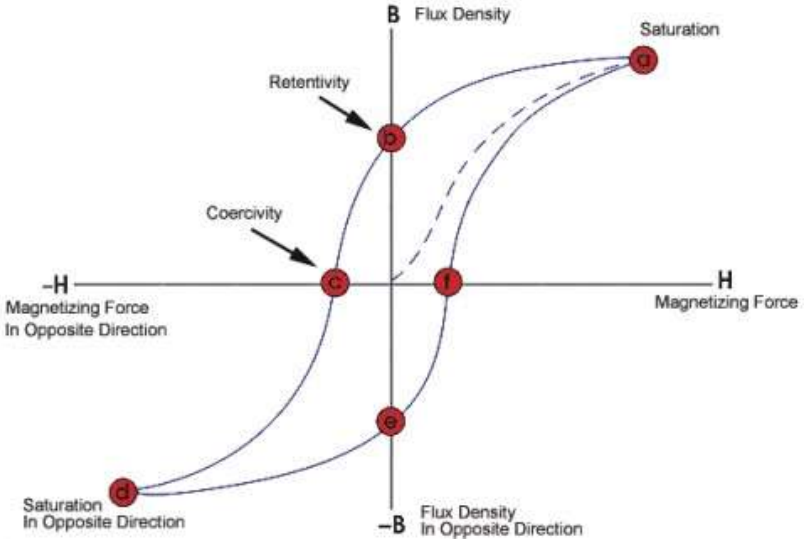

Figure 3.2 Example of a B-H loop with important regions labeled..

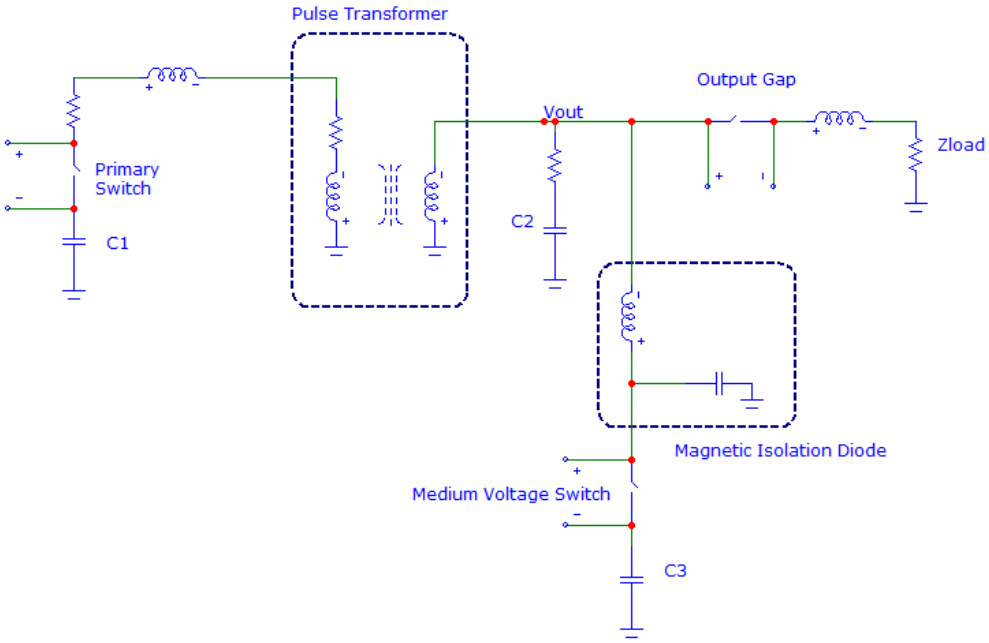

Figure 3.3 Schematic of magnetic isolation diode.

Selection of core material is imperative for this operation in that for repetitive operation the full B-H loop is traversed. Thus losses for the assembly would be determined by the losses in the windings and the losses in the cores due to the B-H loop excursion.

As shown in the example above, the magnetic diode allows for a high voltage pulse to be generated by a step-up transformer. This pulse would be for the purpose of breaking down a gas or striking an arc. The keep alive circuit for the arc or gas discharge is created by the magnetic isolation diode, the medium voltage switch, and C3. The unsaturated inductance of the magnetic diode and C4 allow for a low pass filter to be created such that the medium voltage switch never experiences the high voltage output pulse. The B-H loop for the switch is timed such that the high voltage pulse drives the switch almost completely into saturation, after which the arc ignites the output gap and C2 discharges to zero; the medium voltage switch then closes and C3 pushes the diode into full saturation. At this point, C3 can now discharge through the saturated (low) inductance of the magnetic diode into the load.

This archetype is similar to many parallel pulse compression transformers that are available except that here a small high voltage transformer does not have to carry the high energy discharge current for a low impedance keep alive. Separating the two functions, high current and high voltage, allows for a more optimum design in this case.

3.3 Pulsed Primary Switch

The pulsed primary switch topology works very similarly to the parallel magnetic compression circuit, although it lacks the typical primary switch. The system also utilizes the full energy transfer in a single pulse rather than in two different impedance pulses. During operation Cresonant is charged via pulse charging. The time it takes to charge should be the Vt constant of

the magnetic switch. A diode should also be installed to ensure that current flows in only the intended direction and not back to the pulse modulator that charges the resonant capacitor.

The benefit of this system is not readily clear at first glance. The reader may ask why one would not just utilize the pulse modulator for pulsing the transformer primary in the first place. The rationale behind this is due to the reality of the situation - the system will likely be installed with the modulator topside and the pulse transformer and all associated circuitry located downhole, with at least 5,000 feet of cable between them. Pulse fidelity, especially for shorter pulses, becomes hard to maintain through this kind of charged line connecting the two systems.

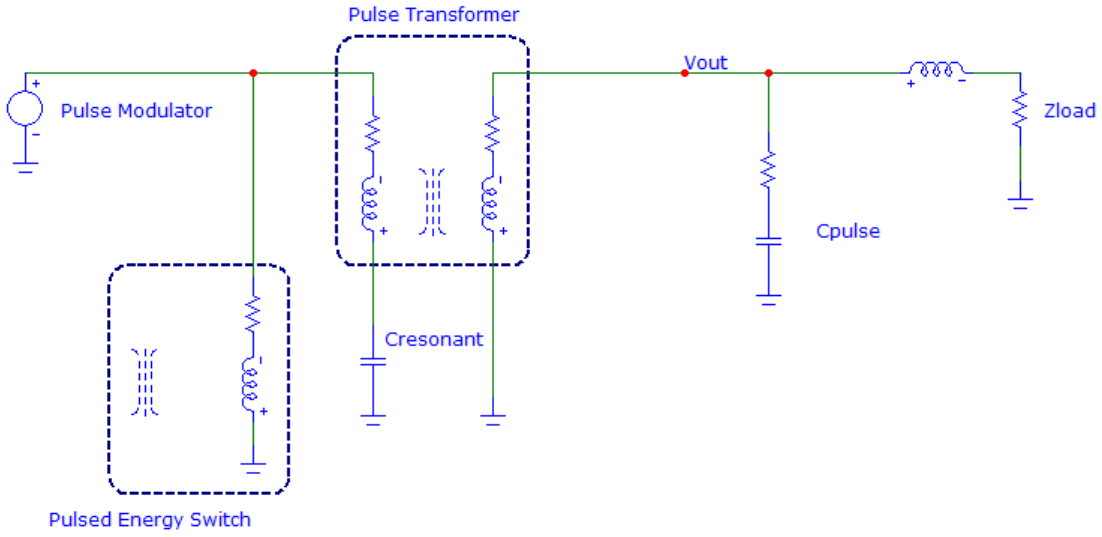

Figure 3.4 Schematic of the pulsed primary switch.

Earlier designs were utilized with the concept of utilizing a thyratron to switch a pulsed charge capacitor downhole. This later design was drawn up when the realization of the enormity of putting a vacuum-based device in the hazardous downhole environment became clear.

3.4 Magnetic Delay Trigger

Modern active devices can be utilized in extreme environmental conditions with great care and extraordinary design effort. Most of these devices require ancillary subsystems to allow for reliable triggering. When utilizing a switch where it must fire after its connected capacitor is pulsed charged, a very simplistic magnetic delay switch can be utilized to generate the voltage at the required timing for triggering of the switch.

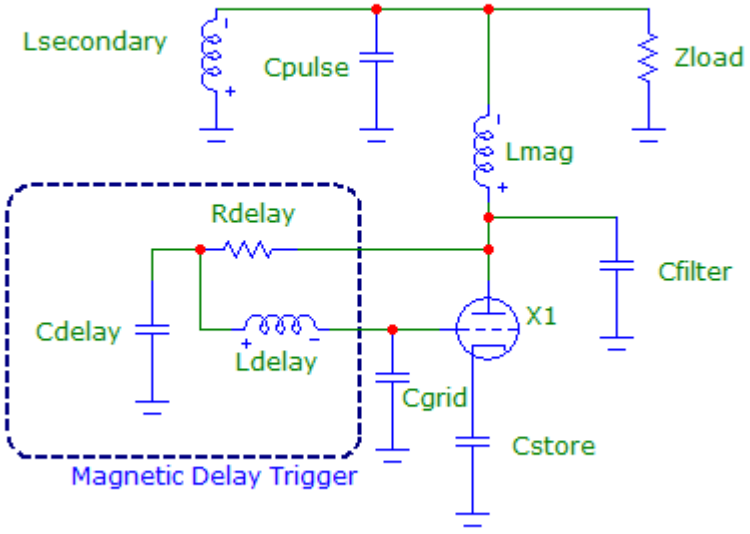

Figure 3.5 Schematic of the magnetic delay trigger circuit.

The schematic in Figure 3.5 illustrates the basic components pertinent to the magnetic delay trigger. For a secondary side switch, as used in the magnetic diode circuit, the designer must provide an isolated, floating trigger that is capable of being in proximity to a high voltage discharge pulse and the high energy discharge pulse. This can be quite a task, especially for a tube-based system. Thyratron tubes are known to experience high grid spike voltages equal to up

to two times the hold-off voltage that the tube experiences. The designer normally incorporates layer upon layer of protection devices such as varistors, transient voltage protectors, spark gaps, and high voltage diodes to keep the active trigger circuitry isolated from these problematic events.

The magnetic delay trigger eliminates the need for these protection elements due to the complete lack of any active components. Ldelay is a small Vt magnetic switch which utilizes the RC time of Rdelay and Cdelay to set a delay time to trigger. This delay time is set by the designer and based upon how long after the initial high voltage pulse he wants the switch to fire. Once the time has elapsed, Ldelay saturates and resonantly charges the grid capacitance (Cgrid) to the required output voltage for trigger generation. Due to the fact that Cgrid is so small, Cdelay can be sized to utilize most of its energy in a voltage gain mode. The main drawback of this topology is that if the pulse-to-pulse repeatability of the output voltage varies over a wide range one can expect to see a large jitter value on this trigger output. Due to the end use for this particular pulse power modulator, the expected jitter is expected to be well within tolerable levels.

3-5 Summary

This chapter presented four different uses of magnetic switching. These applications range from parallel pulse compression, magnetic isolation of lower voltage switches, primary switch replacement, and magnetic delay triggering. Each circuit's benefits and challenges were presented.

The next chapter discusses the simulation of the circuits suggested above and expounds upon the theory of operation for each circuit.

Chapter 4

Simulation Results

4.1 Calculations

Calculations for each design were completed after a suitable Excel chart was crafted. This chart can be viewed in Table 2. It allows the designer to enter in all of the pertinent material characteristics along with pulse requirements to come up with a suitable value for core material.

After this value is created it also gives approximations for saturated and unsaturated inductance based upon the geometry of the winding and the permeability of the magnetic material in a saturated and unsaturated state. The latter are based on assumptions that the material almost completely saturates ($\mu r < 4$).

4.2 Parallel Magnetic Compression

Simulation of the parallel magnetic compression circuit can be seen in Figure 4.1. The initial discharge is rated for 10 J of energy transfer while the remaining energy (1 kJ) was stored in the low impedance secondary energy storage capacitance. As one can see from the simulation, the secondary of the transformer rings the energy into the secondary capacitor (C2) and then initiates the discharge breakdown in the secondary output gap. From here the secondary has a total of 180 kV across the winding, 30 kV from the secondary energy store and -150 kV from the output pulse charging of C2. This results in the saturation of the secondary winding and collapse of the inductance of the secondary. The energy stored in Cpulse now has a low impedance path through to the load impedance. Utilizing the simulation software to double check the calculated Vt constant is helpful in verification of the design before build.

Table 2. Magnetic switch Excel calculator.

Magnetic Switch Design Spreadsheet				
Circuit Parameters				
Core Material Specifications				
	Type =	2605 SA1	Metglas	
	Bsat =	1.59	Tesla	
	Br =	1.36	Tesla	
	Metglas I.D. =	4.00	inches	
	Metglas O.D. =	6.50	inches	
	Metglas width =	1.00	inches	
	Metglas area =	1.25	sq-inches	
	Packing fraction (Metglas) =	0.83	(datasheet)	
Core Parameters				
	Width in inches =	1.0	0.025	meters
	Outer diameter in inches =	6.5	0.165	meters
	Inner diameter in inches =	4.0	0.102	meters
	Area in sq inches =	1.25	8.065E-04	sq meters
	Packing fraction (Metglas/core) =	1.00		
	Overall packing fraction =	**0.83**		
	Area in square inches =	1.25	8.065E-04	meters^2
	Area*PF =	1.04	6.694E-04	meters^2
	Mean radius in inches =	2.63	6.668E-02	meters
	Magnetic path length, Al (inches)=	16.49	4.189E-01	meters
	Single core volt-sec product =	1.97E-03	volt-seconds	
Required Number of Cores				
	Desired # of turns =	10.0		
	Required volt-sec product =	7.50E-01	volt-sec	
	Number of cores required =	**38**		
	Total length of cores =	**38**	9.648E-01	meters
	Total area of cores in sq iunches =	**47**	3.063E-02	sq meters
	Total area*PF = =	**39**	2.542E-02	sq meters
	Inductance Calculations			
	$L \cong 0.002 N^2 h \ln\left(\frac{r_2}{r_1}\right) \mu H$			
	Unsaturated	15738.1	uH	
	Saturated	28.10367822	uH	

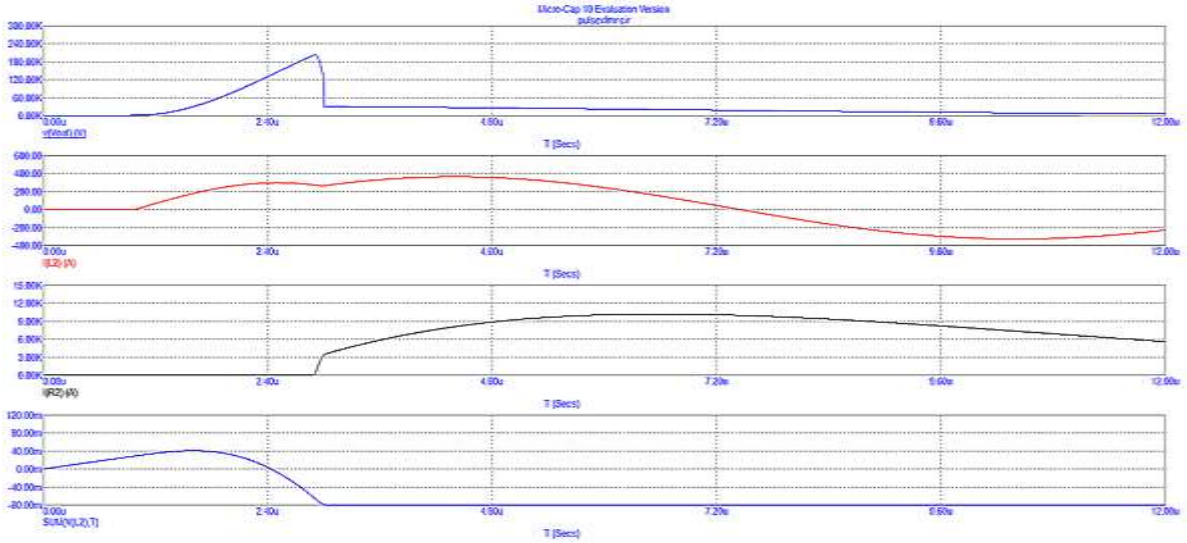

Figure 4.1 MicroCap simulation of parallel magnetic compression circuit.

4.3 Magnetic Diode

Simulation of the magnetic diode circuit is shown in Figure 4.2. As the reader can see the current through the magnetic switch (bottom trace) kicks in after the main discharge occurs and carries the majority of the transferred energy. The initial discharge has a high peak current for a very short period of time, which results in a low (sub-50 J) energy transfer. The higher energy, compared to the parallel magnetic compression circuit, was incorporated as a means to keep the arc alive while the magnetic diode falls into saturation.

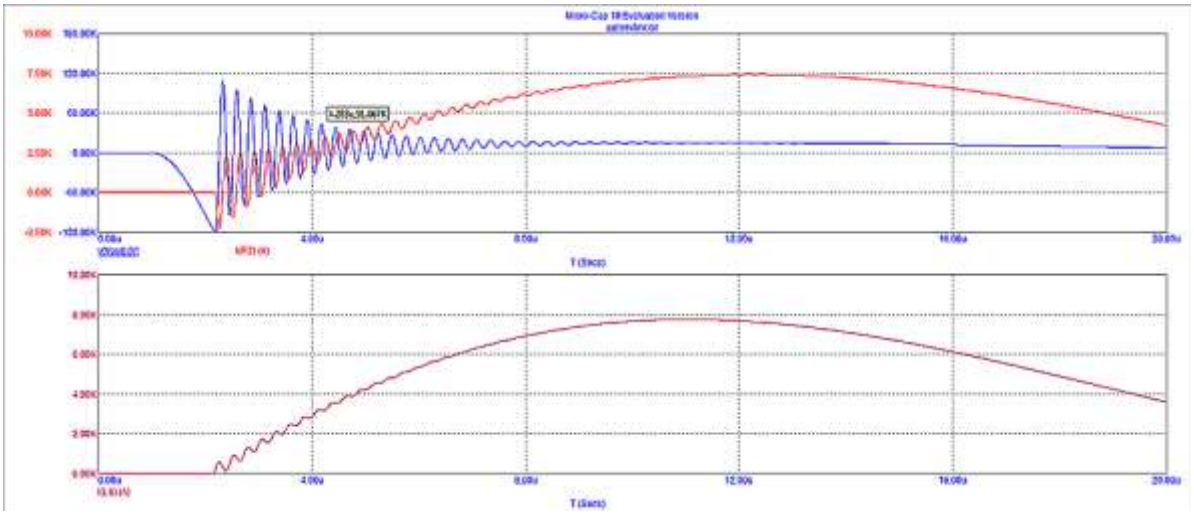

Figure 4.2 MicroCap simulation of the magnetic diode circuit.

One can also see in Figure 4.3 that the voltage impressed upon the anode of the energy discharge switch stays well within the limits of the switch (< 5 kV). The summation of the applied voltage over time comes to an appropriate value for the calculated total in the spreadsheet.

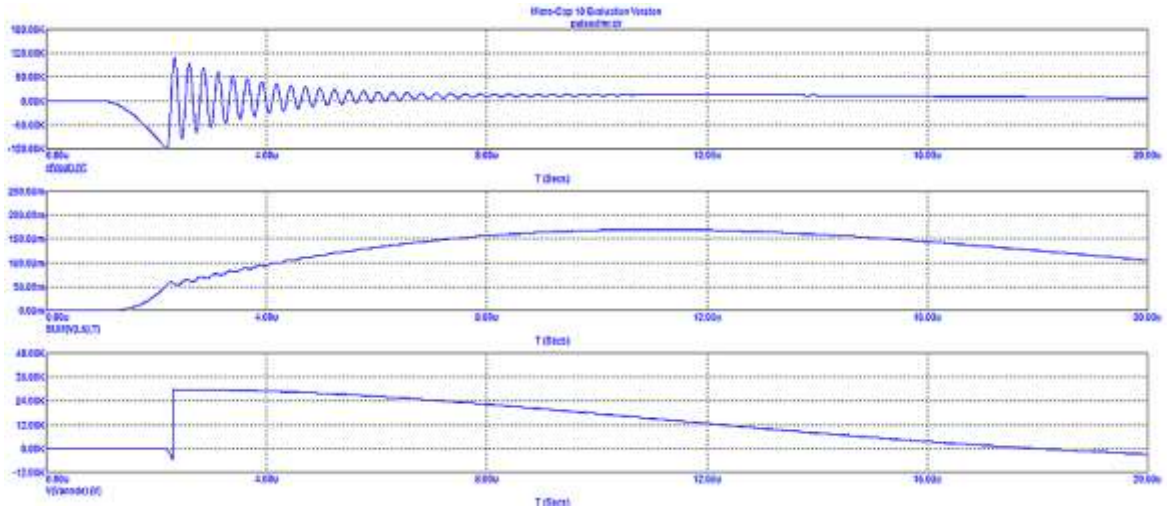

Figure 4.3 MicroCap simulation of the magnetic diode circuit showing isolated switch voltage and Vt constant.

4.4 Pulsed Primary Switch

The schematic in Figure 4-4 and associated simulation in Figure 4-5 show the general format and operation of the circuit. Voltage source C5 pulse charges C4 through L11, which represents the cable inductance. L10 is both the unsaturated and saturated inductances of the magnetic switch due to being controlled by the Jules-Atherton model expression. This expression allows the use of nonlinear magnetics and simulation of saturation of magnetic components. A description of its use is presented in Appendix 2. L1 and L2 make up the transformer primary and secondary. C3 is the secondary energy store. As one can see, the downside to this circuit is the amount of core material necessary for the magnetic switch and the transformer. The advantage of this circuit is that is requires absolutely no active circuitry.

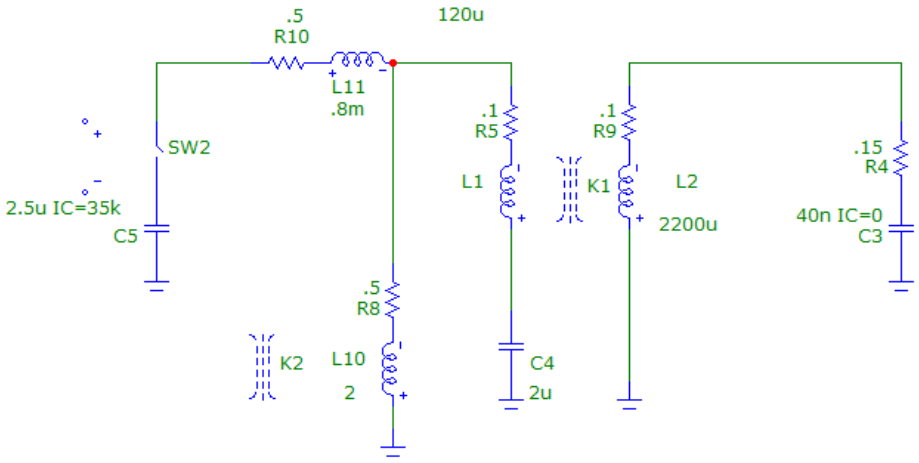

Figure 4.4 Schematic of the pulsed primary switch.

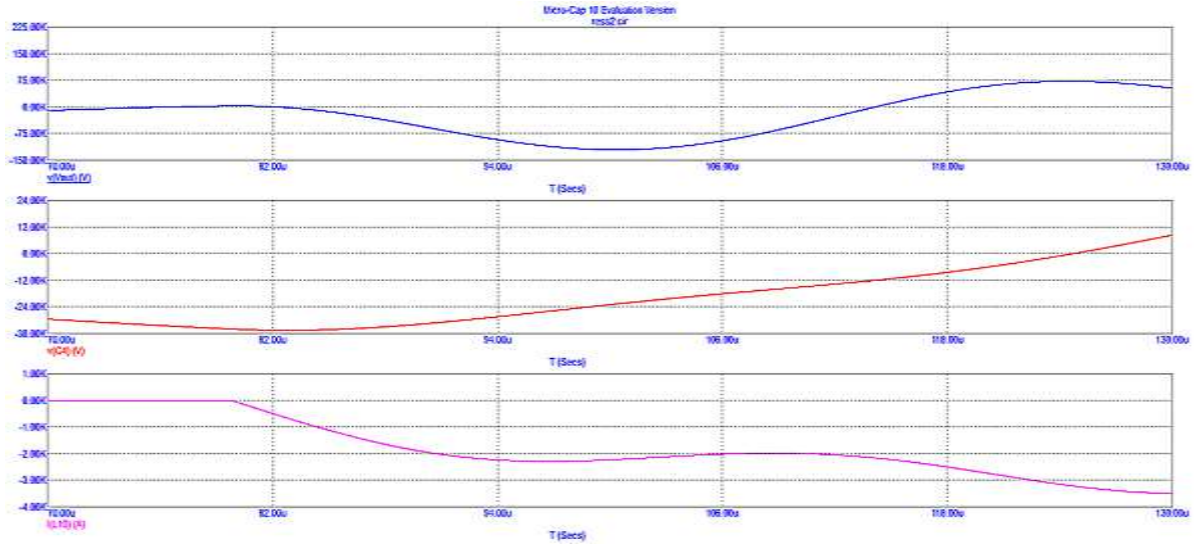

Figure 4.5 MicroCap simulation of the pulsed primary switch.

As the reader can see the Vt of L10 is set to the peak charge voltage on C4. Once C4 is charged L10 saturates which transfers the energy through the primary of the pulse transformer.

4.5 Magnetic Delay

The simulation of the magnetic delay circuit can be viewed in Figure 4.6. As shown the voltage on Cdelay comes up to peak value with the timing of the voltage on the output pulse. At this point in time the magnetic switch (Ldelay) saturates and charges the grid capacitance of the thyratron tube.

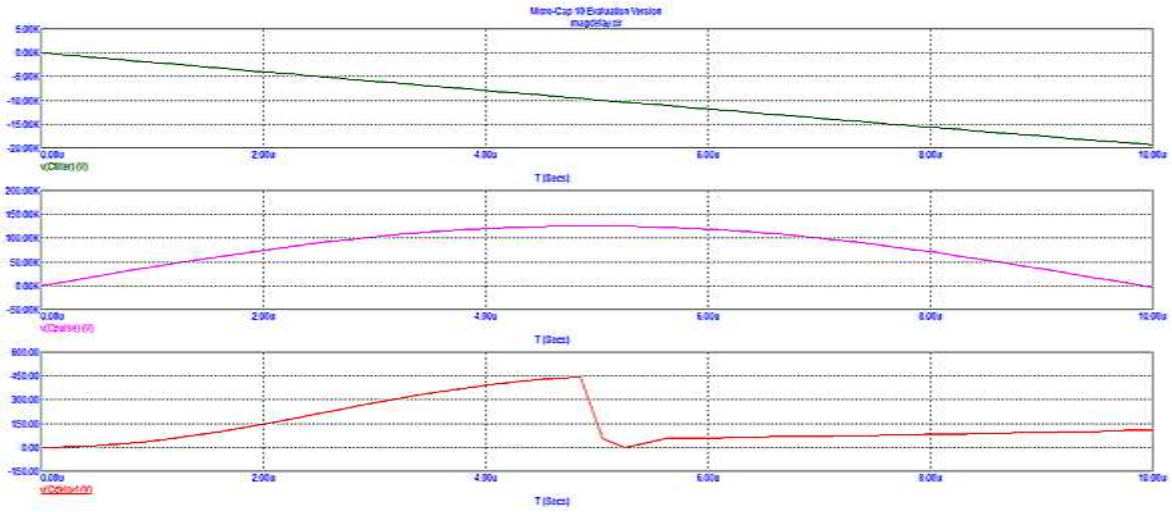

Figure 4.6 Simulation of the magnetic delay circuit

4-6 Summary

This chapter covered the simulation of each of the practical application circuits as they would be implemented in system. The waveforms from the simulation were illustrated along with some of the challenges uncovered during the simulation process.

The next chapter presents the build of each of the solutions along with challenges and lessons learned for each of the circuits.

Chapter 5

Experimental Setup

5.1 Parallel Pulse Compression

The initial transformer was designed for a short pulse stepping up a 30 kV primary voltage to a 150 kV secondary. Due to concerns about lamination voltage holdoff, it was constructed out of 28 one inch-thick Metglas cut C cores. The trade-off between ease of assembly and saturated μr for a cut C core versus toroid was made in favor of the C core. Figure 5.1 shows the completed assembly with an integrated E dot probe mounted to the output side.

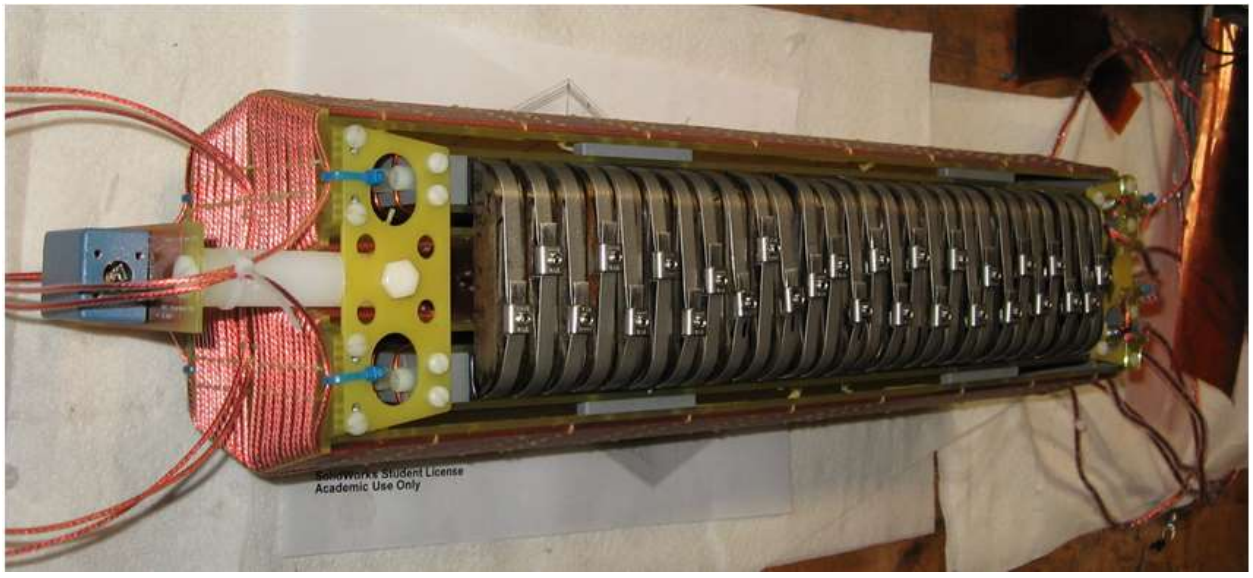

Figure 5.1 Final build of the saturating transformer.

The windings were shaped in bipyramidal fashion into order to mitigate high fields on the winding structure. The winding structure was made from G10 and the windings were held in place by stitched waxed threading. This was to ensure that the windings stayed in place during the high energy discharge. Earlier versions had issues with turn-to-turn breakdown due to the

magnetostriction of the wire during the high *di*/*dt* discharge event. Figure 5.2 illustrates actual winding structure and its 3D design.

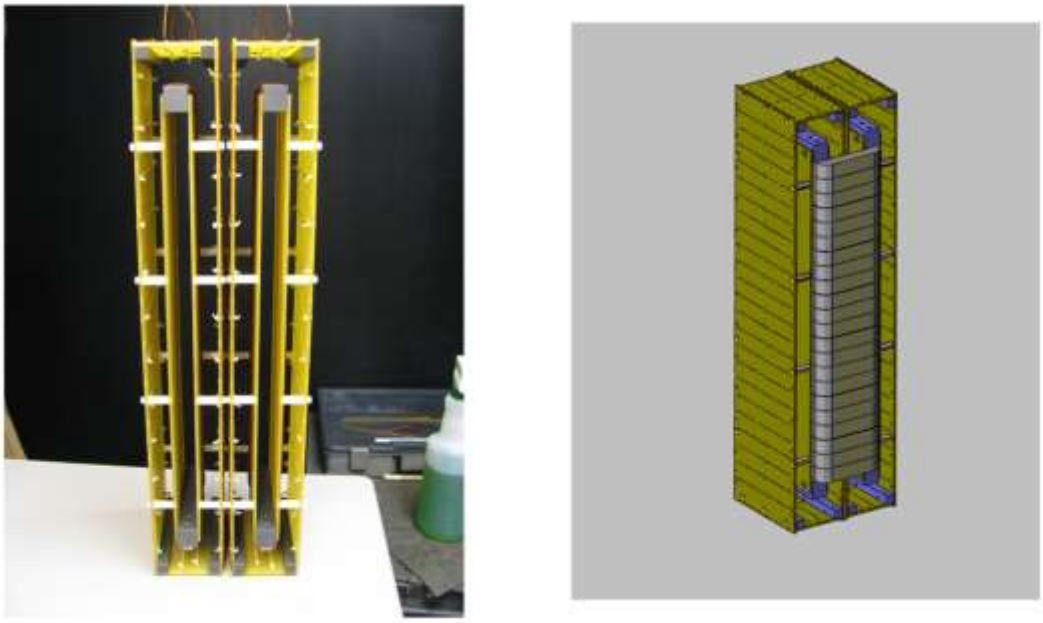

Figure 5.2 Initial build of winding structure (left) and its 3D design (right).

Figure 5.3 Winding structure turns and their isolation.

5.2 Magnetic Diode

The initial experiment was based on a 1 kJ system isolating a 1 μs long 150 kV high voltage pulse from a 44 kV thyratron. To do this, a small 12-turn MnZn ferrite core saturating switch was constructed as shown in Figure 5.4. The windings were constructed utilizing hard copper pipe and fittings. The whole assembly was immersed in Diala AX transformer oil for insulation.

Figure 5.4 Photograph of the 12-turn MnZn saturating switch.

The magnetic switch was instrumented with a variable reset power supply to allow Brem to be adjusted from the origin on the B-H loop, all the way down to Brem. Pearson current transformers were also mounted in line with the device and separately on the transformer to allow one to view both the initial discharge current and also the current through the high energy discharge path.

5.3 Pulsed Primary Switch

The pulsed primary switch was constructed to allow for testing of the magnetic switch as a primary side switching element. One of the main benefits of this approach is that it allows for an active device replacement with non-active elements. To create the ability to switch for multiple charge voltages, the reset current supply was built to be adjustable. This allows operation with a variable start point on the Brem side of the B-H loop. Since one is able to adjust the delta B of the magnetic switch one can dynamically change the Vt constant of the device. This device was built as a proof-of-principle setup. As such, it was only built to operate at a low repetition rate. The primary windings were not designed for any mode of operation above 1 Hz.

Figure 5.5 Photograph of the final build of the pulsed primary switch.

5.4 Magnetic Delay

A small magnetic delay circuit was constructed and implemented on the magnetic diode pulsed power assembly after numerous failures of the active triggering system occurred. Once the design was

implemented and tuned to the proper values there were no longer any failures in the triggering system. A photograph of the implemented system can be viewed in Figure 5.6.

Figure 5.6 Photograph of the magnetic delay circuit out before installation.

5.5 Summary

This chapter presented the realization of the circuits outlined in previous chapters. Pictures of each system in a final build state were presented. Each of the builds had their own challenges which were discussed.

The next chapter goes through the results from testing the above circuit builds. It touches on the systems the circuits were installed in, as well as the performance of the circuits in system.

Chapter 6

Experimental Results

6.1 Parallel Magnetic Compression

The initial pulse power modulators utilized in these experiments were based around the following parameters:

1) Spark ignition at 150 kV-180 kV
2) Resistive loading that drops exponentially down to 2 Ω
3) Load failure mode 10% of the time where load resistance drops to 0.2 Ω
4) Peak current into a 2 Ω load up to 12 kA
5) Peak current delivery in under 2 μs

The initial parallel magnetic compression circuit was built to these parameters. Follow-on systems had adaptations to the above requirements as the experimental process was refined and further understood. Waveforms from the operation of the parallel magnetic compression system can be viewed in Figure 6.1. The waveforms in Figure 6.1 show the charge voltage of the energy store (blue), the output voltage from the high voltage transformer (magenta), and the output current through the switch action of the secondary (green). As one can see, the high voltage comes up until the discharge occurs. From there the circuit operates in an underdamped oscillation while the energy from the secondary energy store starts to flow through the saturated secondary inductance of the parallel magnetic compression circuit.

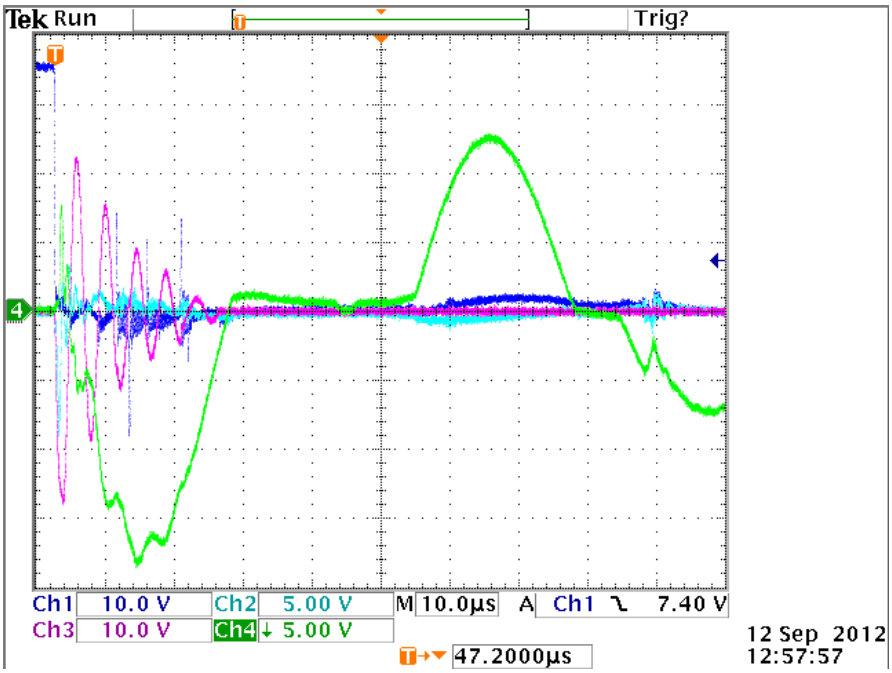

Figure 6.1 Waveforms from the parallel magnetic compression system.

6.2 Magnetic Diode

The system that incorporated the magnetic diode was first designed for a 1 µs pulse. Shortly after this the transformer risetime was extended and thus the magnetic diode had to be redesigned and rebuilt in order to account for the added Vt exposure. The extended waveform from the transformer can be seen in Figure 6.2. Primarily, this was done via adjusting the number of cores in parallel, adjusting the cross-sectional area. Due to the extension of the windings path length, the saturated and unsaturated inductance also grew. This introduced a slight delay in the waveform compared to the parallel pulse compression circuit. This delay can be seen in the waveform shown in Figure 6.3.

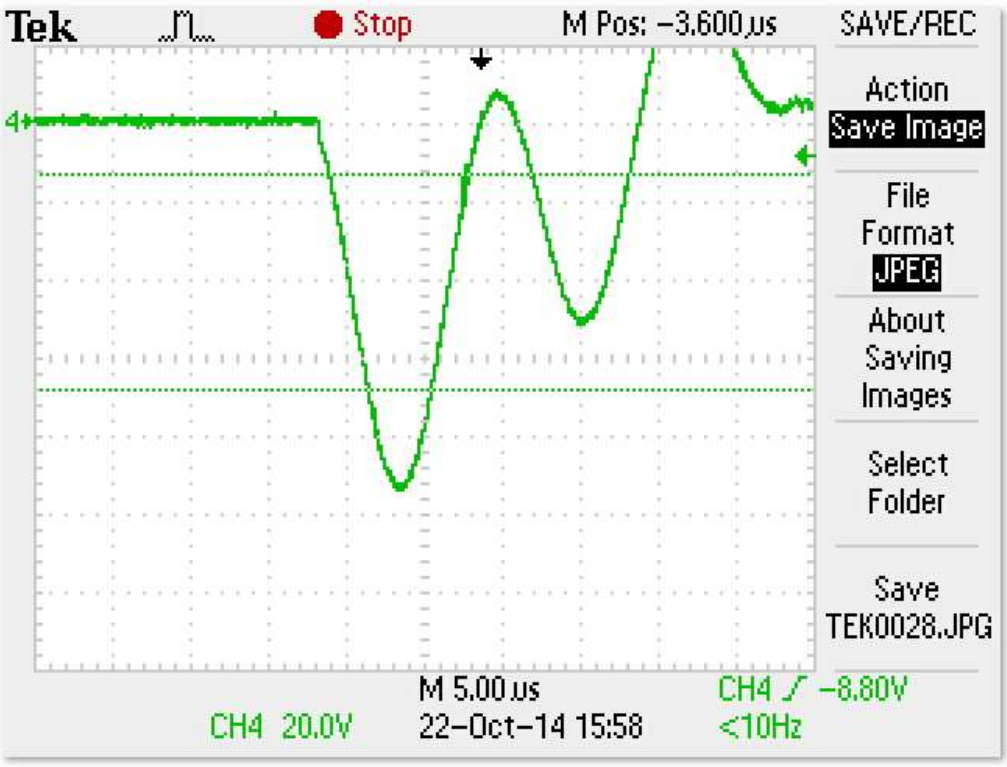

Figure 6.2 Output pulse from extended pulsewidth high voltage transformer.

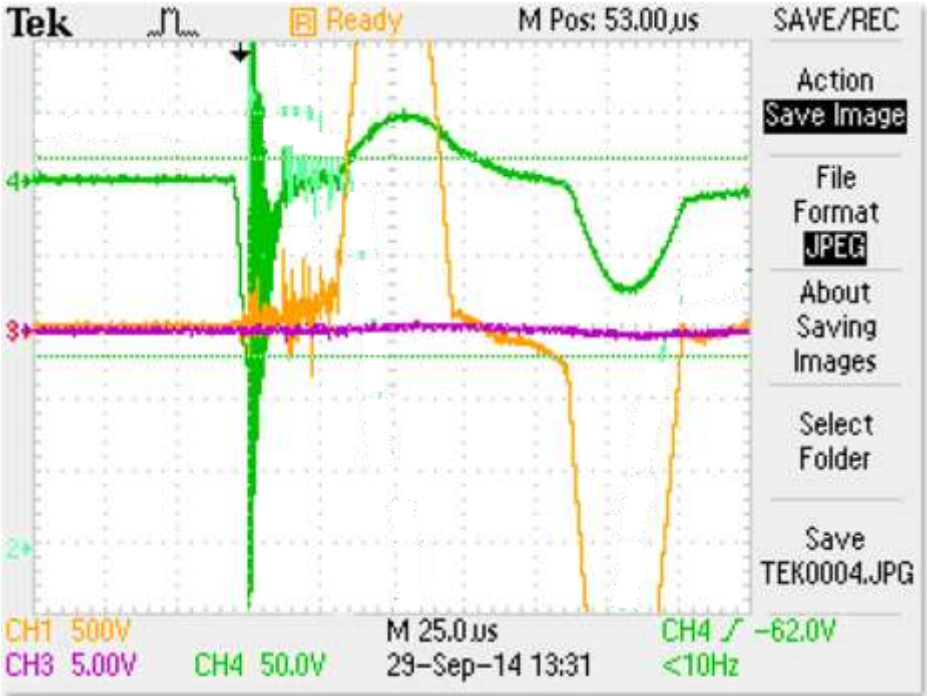

Figure 6.3 Waveforms from the pulse modulator with the magnetic diode installed.

The reader can see the delay in current (orange trace) from the time of breakdown, where the green trace transitions from peak negative voltage to zero. This delay time was later minimized with some effort by adjusting the turns versus cross-sectional area of the magnetic switch.

6.3 Pulsed Primary Switch

The pulsed primary switch was built as a half energy system (500 J). This was done primarily to demonstrate the system as a valid concept. The system was connected to an extended risetime (>10 μs) pulse transformer that was installed on an unused power modulator. The thyratron that was previously installed on that machine was removed along with all of its housekeeping accessory components. Since the machine was previously in a fully operational state the system was immediately able to come up to voltage with no issue. Figure 6.4 shows a waveform from the device operation. Channel one is obtained using a 10,000:1 NorthStar 200 kV voltage probe. Due to its operation this technology is slated for future experimentation and evaluation.

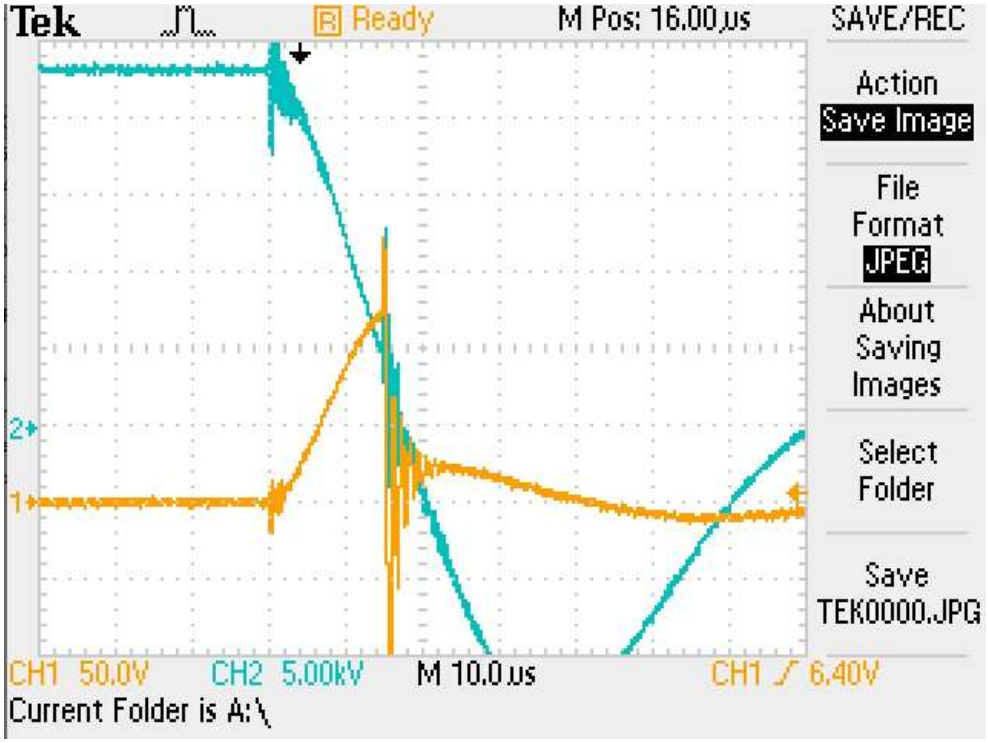

Figure 6.4 Waveform from the pulsed primary switch proof-of-concept.

6.3 Magnetic Delay

The build of the magnetic delay was a simplistic matter. A 3F3 ferrite was obtained and wound to the appropriate number of turns with insulated high voltage wire. This was then connected to a high voltage doorknob capacitor of appropriate value. This small assembly was installed in place of the present high voltage thyratron trigger circuit. The doorknob capacitor would later on have to have a set of trim capacitors added in parallel in order to obtain an optimum output voltage to the grid of the thyratron. Otherwise, the system operated as designed for tens of thousands of shots without any complications.

6-4 Summary

In the above sections the testing of the circuits discussed in earlier chapters was presented. They included difficulties and lessons learned during and after the implementation of the systems. Performance and waveforms from the testing of these circuits was also presented.

The next chapter outlines conclusions based on the design, simulation, build and testing of the above circuits. It also explores options for further research and development for using these technologies.

Chapter 7

Conclusions

7.1 Parallel Magnetic Compression

The parallel pulse compression circuit worked extremely well within the original design parameters. Early versions of this transformer attempted to utilize off-the-shelf magnetic components as used in many power supplies and inverters. Unfortunately, the saturation of these cores proved to be slow and therefore quite lossy. Later designs incorporated custom wound cores to correct for this tendency. These designs were insulated utilizing oxide layers between the layers of nanocrystalline tape. This oxide layer would only handle very small amounts of voltage induced turn-to-turn. The induced voltage was due to eddy current losses from the high dB/dt involved in the switching action. Due to this, the core size had to be broken up and the cores isolated from one another. Further testing revealed a need for the pulsed power system to incorporate isolation of the low impedance charge voltage from the output, a need for a longer risetime, and an extended pulsewidth for the initial discharge circuit. This topology became difficult to modify to fill the new parameters. The need for a downhole active switch also limited the use for this topology in future systems. However, for laboratory use it excelled and was an extremely fault-tolerant system design.

7.2 Magnetic Diode

The utilization of a magnetic diode for the purpose of isolating a lower voltage switch from a high voltage pulse worked well. The faster the risetime and the lower the pulsewidth of the isolated pulse the more effective this solution and less intricate the design can be realized. As

risetime and pulsewidth increase the magnetic diode design must adapt. For designs that must utilize a set footprint the designer is presented with a growing problem from an insulation of the windings standpoint. As for increasing the core material, the path length grows, which increases the saturated inductance. This situation happens for both increases (turns and cross-sectional area) such that the turn-on delay and peak current for the output pulse becomes increasingly diminished (for the later) and longer (for the former). Otherwise, the system operates as designed and can operate in situations where other solutions are incapable of operating. If designed with a flowed dielectric utilized for turns isolation, the device can even be operated to complete insulation failure and recover after the failed dielectric is flowed out. This system's use in future designs was also limited by its need for active switching elements downhole.

7.2 Pulsed Primary Switch

The pulsed primary switch is a hard system to design. The designer needs to balance the required primary inductance of the pulse transformer with the saturated inductance and unsaturated inductance of the magnetic switch. The saturated inductance has to be low into order to effectively transmit the energy through the pulse transformer. If the saturated inductance is too high you end up losing a good portion of the charge voltage to inductive division between the pulse transformer primary inductance and the saturated inductance. Meanwhile, the unsaturated inductance has to be quite high in order to not load the charging of the primary energy storage capacitor. For this system design in the field one has the additional concern of having the pulse unit existing at the end of a multi-thousand foot cable. Due to inductive concerns and grounding issues this cable has to be coaxial. Since the high voltage cable is coaxial it is quite capacitive as well. Thus, the designer ends up with a charged line that oscillates in several modes once the topside pulse launches the charge voltage down the line. A clever designer can utilize these

modes as a sort of resonant frequency charging gain in order to compensate for the overall losses of the system. Since this system was primarily proof-of-concept it was only tested with an inline isolation inductor in the charge line to simulate the inductance of the long cable. The system performed well once additional magnetic material was added such that a wider range of saturation could be affected with the reset current variability.

It is recommended for future designers interested in this topology to utilize an air core, or open core pulse transformer topology similar to that presented in [19]. When designed in this fashion one only has to worry about the magnetic switch saturation and not the pulse transformer.

7.3 Magnetic Delay Trigger

The magnetic trigger circuit performed well for an established system. For systems that are just being brought up, or need to operate over a wide variety of output voltage, especially for low values of total charge voltage, this solution is unlikely to work. The ability to bring up a pulsed power system gradually is an especially strong need due to the large energy and high peak powers involved with their operation. Having to run initial tests at full or near-to-full power is dangerous from a multitude of fronts. As such, they are best utilized on systems that are fully tested and acknowledged to be in full working order. An alternative to this would be to operate the system with a trim capacitance readily available for mechanical adjustment. Once the system is installed it is a robust and extremely fault tolerant solution to high voltage triggering.

7.4 Future Work

Work up to this point has utilized 2605SA1 Metglas due to its availability and relatively low cost. Future work plans involve utilizing higher Bmax materials such as Supermendur and/or Permendur. These materials have the added benefit of operating at extremely high temperatures with little to no change in their permeability and Bmax characteristics. Alternative designs incorporating magnetic switches and magnetically loaded open transformer geometries are also being worked on in order to make use of a minimization of active elements in the pulsed power systems. Systems incorporating Tesla coil-like resonant ring-up have been proposed as well and are being investigated.

7-5 Summary

This thesis explored the use of nonlinear magnetic devices in archetypical pulsed power systems. The application is for the simplification of designs meant to be used for electrocrushing and electrohydraulic drills for extreme environment operation. A number of these designs were simulated, built, and tested. The designs were implemented on a 1-2 kJ pulse modulator built for the purposes of testing a number of effects on various experiments. The modulator was built in a number of fashions in order to experiment with the various architectures made possible by this work. The proven designs were later implemented in a laboratory machine running extensive testing on various solid materials. These successful designs were based upon a parallel magnetic compression circuit, a magnetic diode circuit, a pulsed primary switch circuit, and a magnetic delay trigger circuit.

It is the author's intention to encourage the use of nonlinear devices for use in these harsh environments. Further work was suggested to make use of these devices and systems in future design cycles.

Appendix A

Patent listings from original inception of nonlinear magnetic devices to 1950

Patentee	United States Pat. No.	Filed	Issued	Reason selected
Burgess, C. F., and Frankenfield. B.	720,884	6–12–01	2–17–03	Early d-c saturable reactor. Control circuit decoupling means as follows: series impedance 3-legged and 4-legged cores, hollow annular cores, and magnetic "cross valve" core arrangements.
Crocker, F. B.	891,797	7–25–04	6–23–08	Early d-c saturable transformer. Control circuit decoupling means utilizing a 3-legged core.
Alexanderson. E. F. W.	1.206.643	12–07–12	11–28–16	First to mention gain properties. Early d-c saturable reactor with d-c bias means. Control circuit decoupling means employing two cores, also 4-legged cores.
Osnos, M.	1,227,302	7–08–15	5–22–17	Saturable reactors with 2-core and 3-legged core control circuit decoupling means.
Elmen, G. W.	1,289,418	11–23–15	1–31–18	Early Wheatstone bridge circuit employing signal-controlled reactor in one arm. Novel control means is by controlling the amount of agitating magnetomotive force to obtain variable hysteresis-effect reduction. Hollow annular core for circuit decoupling.
Alexanderson, E. F. W.	1,328,797	11–26–15	1–20–20	Early illustration of external feedback means. Control circuit decoupling means employing two cores, also 4-legged and 8-legged cores.
Alexanderson, E. F. W.	1,328,610	1–21–16	1–20–20	Early to claim off-resonant principle for increased gain. Also frequency discriminating means in a-c power supply and control circuits. Early illustration of cascaded magnetic amplifier stages.
Hartley, R. V. L.	1,462,038	12–30–16	7–17–23	A fundamental push-pull magnetic modulator.
Hartley, R. V. L.	1,287,982	2–16–17	12–17–18	D-c saturable transformer with ultra-carrier frequency magnetomotive force means for hysteresis effect reduction.
Stockle, E. R.	1,376,978	11–24–17	5–03–21	Fundamental d-c saturable transformers with controlled-reluctance shunts; useful embodiments.
Alexanderson, E. F. W.	1,328,473	4–20–18	1–20–20	Means for utilizing a simple winding for the combined functions of saturation control, d-c bias, and as the reactance winding of a d-c saturable reactor.
Jonas, J.	1,434,346	10–04–20	10–31–22	Early full-wave d-c saturable reactor circuit with internal feedback. Control by d-c saturating winding.
Slepian, J.	1,645,302	4–21–21	10–11–27	A magnetic "self-modulator" (amplitude modulator) employing phase-controlled external feedback.
Heising, R. A.	1.654.932	6–29–22	1–03–28	A magnetic "self-modulator" (amplitude modulator) with external feedback.
Heegner, K.	1,656.195	10–23–25	1–17–28	Fundamental negative-resistance type magnetic self-modulator (amplitude modulator). Basic to the general class of magnetic amplifiers with negative resistance characteristics.
Lee, F. W.	Re. 19,129	10–30–26	4–03–34	Early means for obtaining zero output current from a magnetic amplifier in response to zero signal input. One embodiment utilizes "dummy" reactors. Early magnetic amplifier employing, though not claiming, Graetz-connected (full-wave bridge) copper-oxide rectifiers for demodulation.
Thomas, P.	1,734.239	9–23–27	11–05–29	A preferred winding configuration for 3-legged core d-c saturable transformers of Class B′.
Dowling, P. H.	1,739.579	6–20–28	12–17–29	Novel external feedback means comprising center-leg winding shorted by rectifier (for 3-legged cores only). Also novel d-c balancing means in d-c output circuit. Early permanent magnet d-c bias means. Combination circuits.
Dowling, P. H.	1,862.211	6–20–28	6–07–32	External feedback type and ferroresonant type magnetic "self-modulators" (amplitude modulators) in which the modulating frequency is determined by the *R-L* or *L-C* time constant of the control circuit.
Dowling, P. H.	1,878.764	6–20–28	9–20–32	Balanced magnetic amplifier comprising an output transformer with two opposing primary windings one of which is seriesed with the reactance winding of a controlling d-c saturable reactor. Zero stage output for zero control signal.
Peterson, E.	1.884.844	3–30–29	10–25–32	Fundamental negative-resistance type magnetic amplifier.
Dowling, P. H.	1.793.213	11–20–29	2–17–31	Magnetic amplifier comprising a Wheatstone-bridge-shaped core. Bridge balance is affected by controlling the magnetic reluctance of the bridge arms.
Dowling, P. H.	1,910.381	12–26–29	5–23–33	Novel magnetic amplifier type coincidence detector. D-c saturable reactors and transformers in novel combinations.
Sorensen, A. J.	1,824.577	2–07–30	9–22–31	Early Wheatstone bridge type magnetic amplifier. The four reactance arms of the bridge are the four reactance windings on two 3-legged reactors.
Dowling, P. H.	1,891,044	3–25–30	12–13–32	Early counter-acting a-c bias magnetomotive force at power supply frequency; means comprises shorting winding linking d-c control leg. Also novel balanced magnetic amplifier comprising d-c saturable reactor in combination with transformer. Novel core and winding configurations. Early external feedback type flip-flop.

Patentee	United States Pat. No.	Filed	Issued	Reason selected
Dowling, P. H.	1,835,209	6–23–30	12–08–31	D-c saturable reactors and transformers in novel combinations. Novel core and winding configurations are used.
Dowling, P. H.	1,862,212	6–23–30	6–07–32	Series ferroresonant circuit with flip-flop action. Also a novel d-c saturation controlled-balance transformer with opposing secondary windings.
Sorensen, A. J., and Dowling, P. H.	1,914,220	6–23–30	6–13–33	A group of significant and novel push-pull (balanced) magnetic amplifier circuits.
Peterson, E.	1,884,845	9–23–30	10–25–32	Variations on negative-resistance type magnetic amplifier.
FitzGerald, A. S.	1,914,201	10–02–30	6–13–33	Early phase-shift circuit employing a d-c saturable reactor as variable *L*.
Nagashev, B. V.	1,920,803	10–11–30	8–01–33	Wheatstone bridge type magnetic amplifier comprising a single 3-legged core with two bridge arm windings on each of the outside arms of the magnetic core. Bridge balance is affected by d-c magnetomotive force introduced in the center leg.
Sorensen, A. J.	1,862,204	12–06–30	6–07–32	Magnetic amplifier type combination coincidence detector and flip-flop.
Dowling, P. H.	1,842,392	12–12–30	1–26–32	D-c saturable reactors and transformers in novel combinations. Novel core and winding configurations are used.
Suits, C. G.	Re. 20,317	1-21-31	3-30-37	Nonlinear ferroresonant circuits to increase magnetic amplifier control sensitivity.
Zucker, M.	1,851,692	4-17-31	3-29-32	Wheatstone bridge type *R-L* phase-shift circuit employing a d-c saturable reactor as variable *L*. The *R-L* circuit is energized from a center-tapped impedance or transformer.
Logan, F. G.	1,997,179	5-07-31	4-09-35	Early internal feedback magnetic amplifier wherein the amount of positive internal feedback (net unidirectional flux) is controlled by means of a "flux normalizing" or a-c magnetomotive force-controlling impedance paralleled with the rectifier a-c input.
Schmidt, A.	1,921,703	11-13-31	8-08-33	Early multiple-saturation means for affecting the linearity and constancy of the reactance versus d-c control magnetomotive force characteristic of d-c saturable reactors.
Thomas, H. P.	2,016,977	12-01-31	10-08-35	Wheatstone bridge type magnetic amplifier employing peaked-waveform a-c power supply excitation to excite core to saturation. Nonlinear symmetrical resistive devices provide rectification for internal feedback and d-c output signal.
Logan, F. G.	2,068,188	8-03-32	1-19-37	Standard 3-legged core embodiment of internal feedback magnetic amplifier with control by saturating winding to supply d-c load.
Logan, F. G.	2,036,708	8-08-32	4-07-36	Novel d-c load current control scheme wherin a d-c saturable reactor is employed to variably load the secondary of a specially connected transformer, the primaries of which are seriesed with the a-c input of a full-wave rectifier.
Logan, F. G.	1,981,921	8-10-32	11-27-34	Early use of a-c bias at power supply frequency.
Power, J. R.	1,943,088	9-01-32	1-09-34	Wheatstone bridge type phase-shifter with variable *L* and parallel *C* off-resonant phase adjusting means
Boyajian, A.	2,040,684	12-23-32	5-12-36	Magnetic amplifier control circuit sensitivity-increasing means comprising series and parallel nonlinear ferroresonant circuits employing saturating reactors with controlled d-c bias. Where the circuit has leading current, it appears as a nonlinear capacitance, or saturating capacitance.
Logan, F. G.	1,986,112	5-11-33	1-01-35	Magnetic amplifier control-characteristic-exaggerating means comprising positive temperature coefficient resistor in shunt with d-c saturating (control) winding.
FitzGerald, A. S.	2,027,311	6-21-33	1-07-36	Schemes for improving the operation of cascaded magnetic amplifier stages. A reverse d-c bias is used in one embodiment to cancel the quiescent signal from the stage ahead. Also Wheatstone bridge and push-pull magnetic amplifiers.
FitzGerald, A. S.	2,021,099	7-27-33	11-12-35	A magnetic amplifier matrix method for randomly or successively energizing or de-energizing a plurality of loads one at a time from a single pair of d-c controlled inputs.
Antranikian, H.	2,047,609	8-25-33	7-14-36	Novel push-pull magnetic amplifier system employing Class B′ d-c saturable transformers with pulsating unidirectional magnetomotive force applied via primary windings. Internal feedback by rectifiers in secondary circuits, novel means for compensating for rectifier leakage.
Suits, C. G.	1,968,576	9-23-33	7-31-34	Novel external feedback scheme comprising means for variably shunting the feedback circuit input impedance (here the secondary of a current transformer) to make negligible the temperature and aging characteristics of the dry-disc rectifier in the feedback circuit. Also novel embodiments: magnetic self-modulator and cascaded load sequencing circuit.

Patentee	United States Pat. No.	Filed	Issued	Reason selected
FitzGerald, A. S.	2,026,124	12-01-33	12-31-35	A modified Wheatstone bridge type magnetic amplifier capable of reciprocally and mediately indicating two balance conditions to two respective load circuits.
Burton, E. T.	2,164,383	1-29-34	7-04-39	Several "second harmonic" type magnetic amplifiers and binary flip-flops.
FitzGerald, A. S.	2,027,312	7-23-34	1-07-36	Single-sided d-c saturable reactor type magnetic flip-flop with two stable states.
Dellenbaugh, F. S., Jr.	2,175,379	12-31-34	10-10-39	Off-resonant type magnetic amplifier with novel means for inductively coupling the "parallel" C in order to make possible the use of a smaller C; the saturation control windings are utilized in the coupling scheme.
LaPierre, C. W.	2,053,154	3-27-35	9-01-36	Early "second harmonic type" magnetic amplifier. Employs a Class B′ d-c saturable transformer with opposing secondaries. One embodiment is a magnetometer.
Edwards, M. A.	2,432,399	4-24-35	12-09-47	Wheatstone bridge type magnetic amplifier wherein the d-c saturating windings form a control bridge and the reactance windings are the reactance arms in the controlled reactance bridge.
Hanley, S. M.	2,144,289	8-26-35	1-17-39	Novel 3-legged reactor with unbalanced a-c flux path to purposefully create a-c flux in center leg. Control is by d-c saturating winding and by variably shunted winding on center leg. Two-core equivalent is shown.
Edwards, M. A., and Kane, G. A.	2,084,900	10-10-35	6-22-37	Wheatstone bridge type phase-shift circuit employing series L and C in one arm of the bridge.
Dawson, J. W.	2,140,349	10-23-35	12-13-38	Special magnetic amplifier to amplify changes in a-c power supply voltage. This is a simple external feedback magnetic amplifier without a separate control winding *per se*.
Logan, F. G.	2,118,440	3-30-36	5-24-38	Unique a-c bias means for control of special reactor which in turn controls d-c load. A-c control (bias) here is at magnetic amplifier power supply frequency. One-cycle control response is achieved.
Young, H. E.	2,154,020	4-09-36	4-11-39	Differentially balanced magnetic amplifier employing buck-boost d-c saturable transformer or d-c saturable reactor-controlled-transformer in a novel circuit arrangement.
Logan, F. G.	2,126,790	6-23-36	8-16-38	Basic d-c controlled internal feedback magnetic amplifier to control a-c load.
Boardman, E. M.	2,108,642	8-20-36	2-15-38	Two significant push-pull magnetic amplifiers with internal feedback. One of these magnetic amplifiers is of the "second harmonic" type.
Craig, P. H.	2,138,732	9-21-36	11-29-38	Magnetic amplifier control circuit sensitivity-increasing means employing series and parrallel L-C ferroresonant circuit combinations.
Burton, E. T.	2,147,688	12-02-36	2-21-39	Magnetic amplifiers and binary and ternary magnetic flip-flops and delay flop-flops. Some of the devices are of the "second harmonic" type.
Edwards, M.A.	2,169,093	1-02-37	8-08-39	Internal feedback magnetic amplifier to control a-c load. Novel features are d-c bias to compensate for no-load magnetizing flux and capacitor to neutralize load winding reactance. The possibility of a resonant-type magnetic amplifier flip-flop is noted.
Kalbskopf, W.	2,173,905	5-28-37	9-26-39	D-c saturable transformer with opposing secondary windings which are differentially balance-controlled such that the net output voltage is the difference voltage between the two seriesed secondaries. Balanced circuit possibilities exist.
FitzGerald, A. S.	2,168,402	1-11-38	8-08-39	Two single-sided flip-flops combined to form a self-oscillating flip-flop or multivibrator. The flip-flops are cross-connected by their saturation control windings.
O'Hagan, B. E.	2,215,823	6-10-38	9-24-40	D-c saturable transformer having two load energizing secondaries which are mediately and selectively excited in a reciprocal manner according to the amount of coupling of each with the primary as determined by the amount of d-c control magnetomotive force.
Whitely, A. L., and Ludbrook, L. C.	2,229,952	10-19-38	1-28-41	Two novel magnetic amplifiers — one is a nonpolarized magnetic amplifier with internal feedback to control a single d-c load. The other is a polarized magnetic amplifier without feedback to control one d-c load or to reciprocally control two d-c loads.
Hubbard, F. A.	2,218,711	12-30-38	10-22-40	Novel means for the controlled coupling of any one or more of a multiplicity of secondaries to the primary of a d-c saturable transformer. Novel permanent magnet d-c bias means.
Logan, F. G.	2,259,647	2-09-39	10-21-41	Unique a-c bias means for control of special reactor which in turn controls a-c load. A-c control (bias) here is at magnetic amplifier power supply frequency. One cycle control response is obtained.

Patentee	United States Pat. No.	Filed	Issued	Reason selected
Hines, C. M.	2,215,820	6-23-39	9-24-40	Novel embodiment of d-c saturable transformer having two load energizing secondaries the coupling of which to the primary is mediately, selectively and reciprocally controlled by the amount of d-c control magnetomotive force.
O'Hagan, B. E.	2,215,821	6-24-39	9-24-40	Novel embodiment of differentially balanced d-c saturable transformer having opposing secondary windings; the net output voltage is the difference voltage between the two seriesed secondaries. This is a balanced magnetic amplifier.
O'Hagan, B. E.	2,215,822	6-27-39	9-24-40	Novel d-c biasing means for Class B″ d-c saturable transformers.
Geyger, W.	2,338,423	12-14-39	1-04-44	Cascaded Wheatstone bridge magnetic amplifier stages employing novel differentially connected d-c control windings to subsequent stages. Novel external feedback means for Wheatstone bridge magnetic amplifier. Novel Wheatstone bridge output means employing differential transformer.
Hornfeck, A. J.	2,310,955	12-30-39	2-16-43	Push-pull magnetic amplifier employing differentially cross-connected external feedback circuits to reciprocally affect one magnetic amplifier regeneratively and the other degeneratively depending on the polarity of the control signal.
McCreary, H. J.	2,324,634	1-31-40	6-20-43	D-c bias means for use in magnetic amplifiers. Permanent magnet bias means. A-c and d-c magnetic circuit separation and isolation means.
Stevens, S. A., and Walker, A. H. B.	2,222,048	2-21-40	11-19-40	Novel magnetic self-modulators and demodulators.
Krussmann, A.	2,399,872	10-24-40	5-07-46	Wheatstone bridge magnetic amplifier employing only one set of windings which are used for combined functions as d-c saturable control and as the reactance arms of the bridge.
Middel, H. D.	2,388,070	8-22-41	10-30-45	Novel d-c load controlling magnetic amplifier which does not employ rectifiers, but which employs, instead, symmetrical characteristic current distorting impedances which have no rectifying properties *per se*. High magnetic amplifier sensitivity is claimed.
Lamm, U.	2,403,891	9-23-42	7-09-46	Wheatstone bridge magnetic amplifier having external and internal feedback. Also Wheatstone bridge type magnetic flip-flop.
FitzGerald, A. S.	2,464,639	4-13-45	3-15-49	Novel d-c polarized push-pull magnetic amplifier. Novel features include impedance-coupled external feedback means to the control winding instead of to a special external feedback winding. Novel signal-limiters are used to avoid the deleterious effects of excessive control signals.
FitzGerald, A. S.	2,461,046	5-03-46	2-08-49	Novel Wheatstone bridge type magnetic amplifier.
Hedstrom, S. E.	2,509,864	6-19-46	5-30-50	Novel d-c polarized external feedback magnetic amplifier employing push-pull internal feedback magnetic amplifiers.
Forssell, H.	2,504,675	8-21-47	4-18-50	Novel d-c polarized balanced, single ended and push-pull magnetic amplifiers.
Tweedy, S. E.	2,475,575	10-29-47	7-05-49	Novel d-c polarized Wheatstone bridge type magnetic amplifier.
Graves, W. L. O.	2,516,563	4-19-48	7-25-50	Magnetic amplifier for the control of an inductive load. A rectifier limits the negative voltage across the inductive load to establish a mode of operation similar to that for a resistive load.
Lord, H. W.	2,509,738	4-29-48	5-30-50	Novel Wheatstone bridge magnetic amplifier with internal feedback.
Thompson, R. L.	2,519,513	9-09-48	8-22-50	Two-sided magnetic binary counter (flip-flop) with crossed external feedback.
Wood, M. L.	2,524,154	1-05-49	10-03-50	Two-sided magnetic flip-flop with crossed external feedback.

Appendix 2

Utilizing the Jiles-Atherton Model in SPICE

Utilizing the Jiles-Atherton model in SPICE can be a trying effort. There are a number of papers available for the reader to peruse to see how others have calculated the values for the parameters involved in utilizing the model. These models and calculations are quite intensive and difficult for the average designer to produce and use. A much less time consuming solution, and reasonably accurate method, is to simply take an iterative approach to solving the system of multiple variables, i.e., simple trial and error. Unfortunately most SPICE programs do not provide a very good explanation for what each value does so one is left with a time consuming task the first time one wants to simulate a specific magnetic material. Due to this the author has taken the time to put each of these values down and explain what they do to the B-H simulation of a magnetic model.

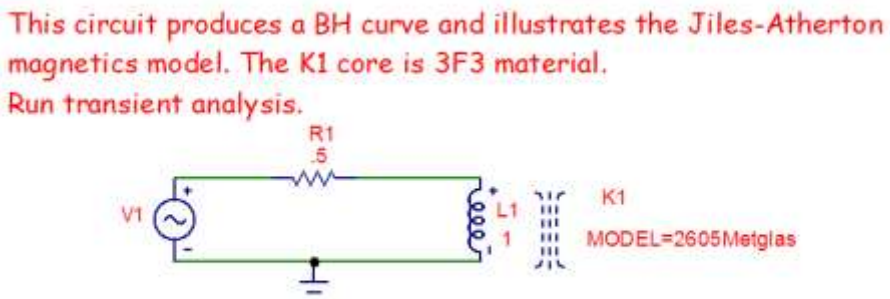

Figure A2.1 CORE.CIR file in MicroCap.

The simulation package utilized here is MicroCap made by Spectrumsoft. One can load their Jiles-Atherton model utilizing the K component and associating a single or multiple inductances to that K. The K component denotes coupling between inductive elements. It can be

used to either couple air core inductors, or couple any number of inductors using a single magnetic core. Once one utilizes a model types (inputting the values for a model) the value typed in for the inductor changes from being the inductance value to the number of turns the inductor has on it. The software takes that along with the other parameters entered (shown in Figure A.2.2) and calculates the inductance utilizing these parameters. One would note that this does not take into consideration a very real aspect of most materials, the pulse permeability. It does, however, allow one to utilize nonlinear effects due to saturation of the core material.

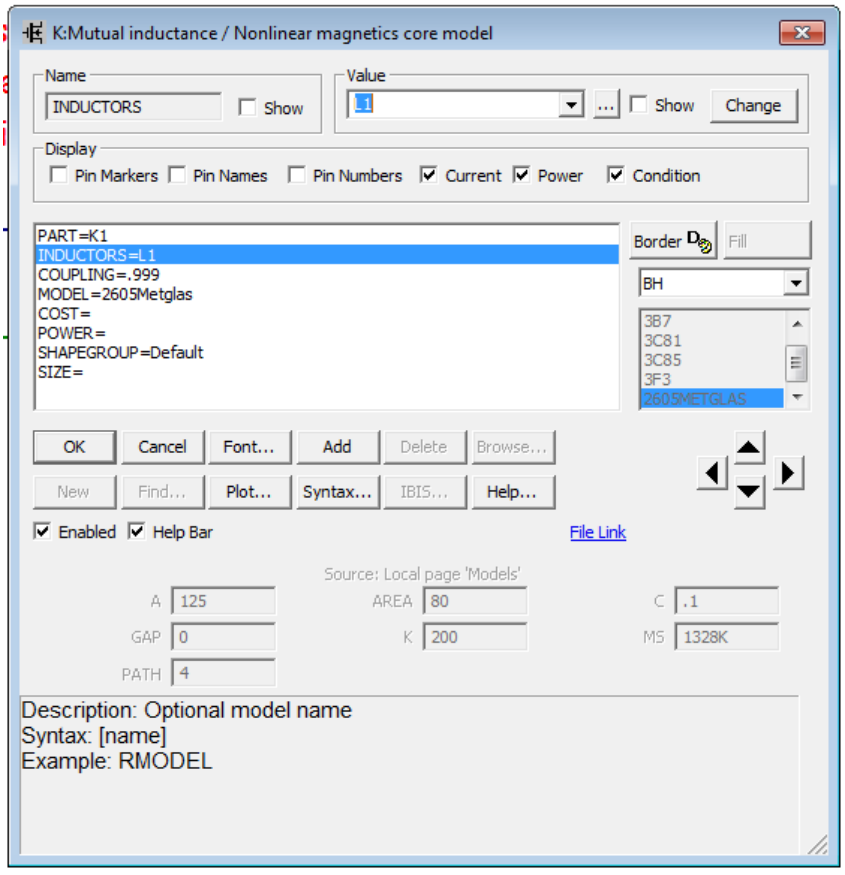

Figure A2.2 Parameters for magnetic modeling.

As shown in Table 3 each of the values in Figure A2.2 are associated with a few parameters of the core material and also how the material responds to magnetic flux. Getting the right parameters for the simulation becomes mostly adjusting C and K values back and forth to get the B-H loop properly shaped. This can be troublesome as they don't seem to change one particular aspect of the B-H loop. Adjusting them individually adjusts the tendency of the loop flexion.

Table 3. Parameters for simulation of magnetic material using the Jiles Atherton model.

Variable	Description	Explanation of Effect	Units
A	Shape Parameter	Adjusts the squareness of the BH Loop. Higher values produce a more transverse characteristic similar to a core in a nonannealed state	A/m
Area	Cross Sectional Area	This value is simply the core cross sectional area, Ac.	cm^2
C	Domain Wall Flexing Value	Utilize this value to adjust the width of the BH loop. Lower values result in a wider delta H	n/a
Gap	Air Gap Length (if any)	Utilize this value to account for any airgap in the core geometry	cm
K	Domain Wall pinning Value	Utilize this value to adjust the width of the BH loop. Higher values result in a wider delta H. Use this value for setting Hmax	n/a
MS	Saturation Magnetization	Use this value to set Bmax. 1000k = 1T or 10kG	A/m
Path	Mean Magnetic Path length	Use this value to set the cores magnetic path length	cm

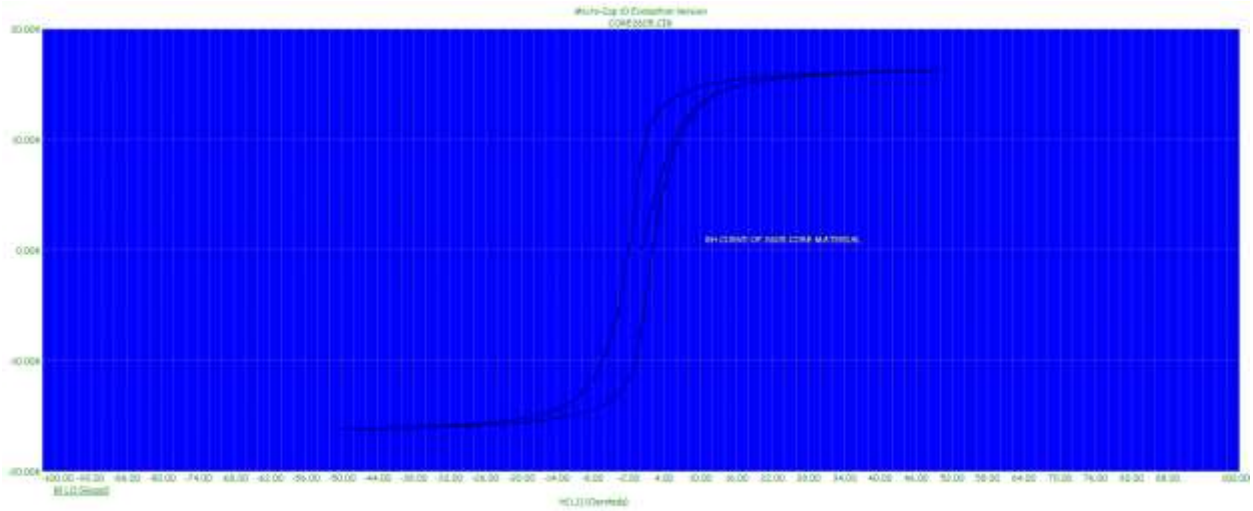

Figure A2.3. Simulation of B-H curve for 2605A Metglas.

REFERENCES

1. C.F. Burgess and B. Frankenfield, “Means for Regulating Self-inductance in Electric Circuits,” C.F. Burgess, B. Frankenfield, assignee. Patent US743444 A. 10 Nov. 1903. Print.

2. C.F. Burgess and B. Frankenfield, “Regulation of Electric Circuits,” C.F. Burgess, B. Frankenfield, assignee. Patent US720884 A. 17 Feb. 1903. Print.

3. S. Platt, *Magnetic Amplifiers: Theory and Application* (Prentice Hall, Inc., Upper Saddle River, NJ, 1958).

4. R.B. Tomer, *Getting the Most out of Vacuum Tubes* (H.W. Sams, Inc., New York, NY 1960).

5. H.D. Sanders and S.C. Glidden, “Compact, High Current, High Voltage Solid State Switches For Accelerator Applications” *Proceedings IPAC2012* (New Orleans, Louisiana, 2012), pp. 3701-3703.

6. H.D. Sanders, S.C. Glidden, and C.T. Dunham, “Solid State Switches For High Frequency Operation As Thyratron Replacements,” *Proceedings IEEE PPPS-2013* (San Francisco, CA, 2013), pp. 546-549.

7. A. Welleman, E. Ramezani, and U. Schlapbach, “Semiconductor Switches Replace Thyratrons and Ignitrons,” *Proceedings IEEE PPPS-2002* (Las Vegas, NV, 2001), pp. 325-328.

8. G. Ravida, O. Brunner, D. Valuch, “Solid State Thyratron Replacement for the LHC Klystron Crowbar,” *Proceedings IPAC2012* (New Orleans, Louisiana, 2012), pp. 3641-3643.

9. R. Beckwith, “Downhole Electronic Components: Achieving Performance Reliability,” *J. Petrol, Tech.* (August, 2013), pp. 42-57.

10. L. Cheng, A.K. Agarwal, C. Capell, M. O’Loughlin, K. Lam, J. Richmond, E. Van Brunt, A. Burk, J.W. Palmour, H. O’Brien, A. Ogunniyi, and C. Scozzie, “20 kV, 2 cm^2, 4H-SiC Gate

Turn-off Thyristors for Advanced Pulsed Power," *Proceedings IEEE PPPS-2013* (San Francisco, CA, 2013), pp. 97-100.

11. S. Waffler, S.D. Round, and J.W. Kolar, "High Temperature (>200◦C) Isolated Gate Drive Topologies for Silicon Carbide (SiC) JFET," *Proceedings IEEE IECON 2008* (Orlando, FL, 2008), pp. 2867-2872.

12. R.S. Pengelly, S.M. Wood, J.W. Milligan, S.T. Sheppard, and W.L. Pribble, "A Review of GaN on SiC High Electron-Mobility Power Transistors and MMICs*," IEEE Trans. Microw. Theory Tech.*, vol. MTT-60, pp. 1764 – 1783 (2012).

13. W.C. Nunnally, "Magnetic Switches and Circuits," Los Alamos National Laboratory Report LA-8862-MS (May 01,1982).

14. E.L. Neau, "High Average Power, High Current Pulsed Accelerator Technology," *Proceedings 1995 IEEE Particle Accelerator Conference* (Dallas, TX, 1995), Vol. 2., pp. 1188-1192.

15. M. Pasnak and R. Lundsten, "Effects of Ultrahigh Temperature on Magnetic Properties of Core Materials," *AlEE Transactions, Pt. I (Communication and Electronics)*, vol. 78, pp. 1033-1039 (1960).

16. RJ. Adler and R.J Richter-Sand, "Advances in the Development of the Nested High Voltage Generator," *Proceedings 1993 IEEE Particle Accelerator Conference* (Washington, DC, 1993), Vol. 2., pp. 1306-1308.

17. R. J. Adler, J. Gilbrech, K. Childers, and E. Koschmann, "A Compact Nested High Voltage Generator for Medium Pulse Duration Applications," *Proceedings 2009 IEEE Pulsed Power Conference* (Washington, DC, 2009), pp. 913-917.

18. Magnetics Inc, “Core Selection for Saturating Transformers,” https://www.google.com/url?sa=t&rct=j&q=&esrc=s&source=web&cd=1&ved=0CB8QFjAAahUKEwilop_379jGAhUQQYgKHaa6DMQ&url=http%3A%2F%2Fwww.mag-inc.com%2FFile%2520Library%2FProduct%2520Literature%2FStrip%2520Wound%2520Core%2520Literature%2Ftwc-s2.pdf&ei=4hWkVaUpkIKhBKb1sqAM&usg=AFQjCNFgierXBBLEZ0Q-dgDF4L5yxXAZ-g&sig2=5mVs5DMvsSbX04mgcDowDA&bvm=bv.97653015,d.cGU (2000).

19. G.J. Rohwein and R.N. Lawson, “An SCR-switched, High Voltage, High Gain Linear Transformer System,” *Proceedings 1989 IEEE Pulsed Power Conference* (Monterey, CA, 1989), pp. 762-765.